0026-895X/05/6805-1254–1270$20.00
MOLECULAR PHARMACOLOGY
Copyright © 2005 The American Society for Pharmacology and Experimental Therapeutics
Mol Pharmacol 68:1254–1270, 2005

Vol. 68, No. 5
15669/3059420
Printed in U.S.A.

Design of PAP-1, a Selective Small Molecule Kv1.3 Blocker, for the Suppression of Effector Memory T Cells in Autoimmune Diseases

Alexander Schmitz, Ananthakrishnan Sankaranarayanan, Philippe Azam, Kristina Schmidt-Lassen, Daniel Homerick, Wolfram Hänsel, and Heike Wulff

Pharmaceutical Institute, University of Kiel, Kiel, Germany (A.Sc., K.S.-L., W.H.); and Department of Medical Pharmacology and Toxicology, University of California, Davis, Davis, California (A.Sa., P.A., D.H., H.W.)

Received June 10, 2005; accepted August 10, 2005

ABSTRACT

The lymphocyte K^+ channel Kv1.3 constitutes an attractive pharmacological target for the selective suppression of terminally differentiated effector memory T (T_{EM}) cells in T cell-mediated autoimmune diseases, such as multiple sclerosis and type 1 diabetes. Unfortunately, none of the existing small-molecule Kv1.3 blockers is selective, and many of them, such as correolide, 4-phenyl-4-[3-(methoxyphenyl)-3-oxo-2-azapropyl]cyclohexanone, and our own compound Psora-4 inhibit the cardiac K^+ channel Kv1.5. By further exploring the structure-activity relationship around Psora-4 through a combination of traditional medicinal chemistry and whole-cell patch-clamp, we identified a series of new phenoxyalkoxypsoralens that exhibit 2- to 50-fold selectivity for Kv1.3 over Kv1.5, depending on their exact substitution pattern. The most potent and "drug-like" compound of this series, 5-(4-phenoxybutoxy)psoralen (PAP-1), blocks Kv1.3 in a use-dependent manner, with a Hill coefficient of 2 and an EC_{50} of 2 nM, by preferentially binding to the C-type inactivated state of the channel. PAP-1 is 23-fold selective over Kv1.5, 33- to 125-fold selective over other Kv1-family channels, and 500- to 7500-fold selective over Kv2.1, Kv3.1, Kv3.2, Kv4.2, HERG, calcium-activated K^+ channels, Na^+, Ca^{2+}, and Cl^- channels. PAP-1 does not exhibit cytotoxic or phototoxic effects, is negative in the Ames test, and affects cytochrome P450-dependent enzymes only at micromolar concentrations. PAP-1 potently inhibits the proliferation of human T_{EM} cells and suppresses delayed type hypersensitivity, a T_{EM} cell-mediated reaction, in rats. PAP-1 and several of its derivatives therefore constitute excellent new tools to further explore Kv1.3 as a target for immunosuppression and could potentially be developed into orally available immunomodulators.

Potassium (K^+) channels in humans are encoded by an extended superfamily of 76 genes (Gutman et al., 2003). Each K^+ channel has a unique expression pattern that allows cells to "fine tune" their membrane potential and their excitability according to their respective functions. Specific K^+ channel modulation therefore offers an enormous potential for the development of new drugs. One channel that constitutes an especially promising target is the voltage-gated Kv1.3 channel. Homomeric Kv1.3 channels are found in human T and B lymphocytes and their expression is up-regulated in terminally differentiated effector memory T cells (Wulff et al., 2003b) and class-switched memory B cells (Wulff et al., 2004). Kv1.3 blockers have therefore been proposed as potential new therapeutics for the treatment of autoimmune diseases (such as multiple sclerosis, type-1 diabetes, psoriasis, rheumatoid arthritis, transplant rejection, graft-versus-host disease, Sjögren's syndrome, and systemic lupus erythematosus) in which effector memory T cells and/or class-switched memory B cells are involved in the pathogenesis (Markovic-Plese et al., 2001; Hansen et al., 2002; Viglietta et al., 2002; Wulff et al., 2003b; Dorner and Lipsky, 2004; Fasth et al., 2004; Vissers et al., 2004; Yamashita et al., 2004; Pearl et al., 2005). In proof of this hypothesis, the Kv1.3 blocking peptides kaliotoxin (Beeton et al., 2001a), ShK (Beeton et al., 2001b), and its recently identified more specific derivative ShK(L5) (Beeton et al., 2005) have been shown to treat experimental

This work was supported by a Pilot Project Grant from the National Multiple Sclerosis Society (to H.W.) and funds from the University of California, Davis.

A.Sc. and A.Sa. contributed equally to this work.

Article, publication date, and citation information can be found at http://molpharm.aspetjournals.org.
doi:10.1124/mol.105.015669.

ABBREVIATIONS: 5-MOP, 5-methoxypsoralen; DMSO, dimethyl sulfoxide; CP-339818, 1-benzyl-4-pentylimino-1,4-dihydroquinoline; UK-78282; 4-[(diphenylmethoxy)methyl]-1-[3-(4-methoxyphenyl)propyl]-piperidine; DTH, delayed type hypersensitivity; 5-HOP, 5-hydroxypsoralen; HEK, human embryonic kidney; NMDA, *N*-methyl-D-aspartate; MOPS, 3-morpholinopropanesulfonic acid; PBMC, peripheral blood mononuclear cells; Ab, antibody; SAR, structure-activity relationship; PAP, phenoxyalkoxypsoralen; ShK, *Stichodactyla helianthus* toxin.

autoimmune encephalomyelitis, an animal model for multiple sclerosis. Kv1.3 has been further validated as a target for the treatment of multiple sclerosis by the demonstration that myelin-reactive T cells in the blood from patients with multiple sclerosis are predominantly Kv1.3^{high} effector memory T cells (Wulff et al., 2003b). Contrary to the aforementioned peptides, a small-molecule Kv1.3 blocker would have the advantage that it could be taken orally.

The first small molecules that were found to inhibit the Kv channel in human T cells were the classic Kv channel inhibitors 4-aminopyridine and tetraethylammonium, the Ca^{2+}-activated K^+ channel blocker quinine, and the Ca^{2+} channel inhibitors verapamil, diltiazem, and nifedipine (for recent reviews, see Wulff et al., 2003a; Chandy et al., 2004). After the cloning of the *Kv1.3* gene in the early 1990s (Grissmer et al., 1990), several pharmaceutical companies started screening their libraries for more potent and more selective small molecule Kv1.3 blockers and identified a number of compound classes that roughly fall into two groups: 1) typical combinatorial library compounds, such as the iminodihydroquinoline CP-339818 (Nguyen et al., 1996), the benzylpiperidine UK-78282 (Hanson et al., 1999), the cyclohexyl-substituted benzamides (Schmalhofer et al., 2002), and the sulfamidebenzamidoindanes (Wulff et al., 2003a), which are of a relatively simple structure and low molecular weight and rich in nitrogen and halogen atoms, and 2) natural products or natural product derivatives, such as the triterpenoid correolide (Hanner et al., 1999) and the candelalides (Singh et al., 2001), which are rich in oxygen atoms and have a more complex stereochemistry. Although some of these compounds are quite potent Kv1.3 blockers, with EC_{50} values of 30 to 200 nM, they all lack the required selectivity over other ion channels, especially the closely related Kv1 family channels.

In contrast to the high-throughput screening approaches applied by pharmaceutical companies, we took an approach that is termed "retroactive exploitation of observations made in man" (Wermuth, 2004). Following up on anecdotal reports that tea prepared from the leaves of *Ruta graveolens,* the Common Rue (Herb of Grace), alleviated the symptoms of multiple sclerosis (Bohuslavizki et al., 1993) we extracted *R. graveolens* and identified a number of Kv1-family channel blocking psoralens and furoquinolines in this plant (Bohuslavizki et al., 1994). In subsequent single-case "off label" trials, the psoralen 5-methoxypsoralen (5-MOP; Fig. 1A), one of the major K^+ channel blocking compounds of *R. graveolens* (Bohuslavizki et al., 1994), was found to improve the functional deficits in multiple sclerosis patients (Bohuslavizki et al., 1993), but its phototoxic activity and its low affinity to Kv1.3 precluded its use as a therapeutic for multiple sclerosis. We therefore started a traditional medicinal chemistry program to improve the potency and selectivity of the psoralens for Kv1.3 and identified 5,8-diethoxypsoralen (EC_{50}, 10 μM) (Wulff et al., 1998), 6-(2,5-dimethoxyphenyl)-psoralen (EC_{50}, 700 nM) (Wernekenschnieder et al., 2004), and Psora-4 (EC_{50}, 3 nM) (Vennekamp et al., 2004). Psora-4 (Fig. 1A), our most potent compound, was 17- to 70-fold selective for Kv1.3 over other Kv1 family channels, except for the cardiac channel Kv1.5 (EC_{50} ~8 nM), raising concerns about potential side effects in vivo.

In the present study, we describe how we have used Psora-4 as a template and have successfully separated the affinities for Kv1.3 and Kv1.5 through further derivatization. Our new psoralen Kv1.3 blocker phenoxyalkoxypsoralen-1 (PAP-1) exhibits 23-fold selectivity over Kv1.5, potently suppresses the proliferation of human T_{EM} cells in vitro, and prevents delayed type hypersensitivity (DTH) in rats when administered intraperitoneally or orally.

Materials and Methods

Chemistry. 5-MOP was purchased from Aldrich Chemical Co. (Milwaukee, WI) and dealkylated with magnesium and iodine at 165°C (Schoenberg and Aziz, 1953) to obtain 5-hydroxypsoralen (5-HOP).

General method A. 5-HOP was reacted with the respective alkyl halides in the presence of an excess of anhydrous potassium carbonate and catalytic amounts of potassium iodide under reflux in a dry organic solvent. The progress of the reaction was monitored by thin-layer chromatography. After completion of the reaction, the crude product mixture was diluted with water and acidified to pH 1 with concentrated hydrochloric acid. The aqueous slurry was extracted with dichloromethane. The organic phase was washed first with 1% sodium hydroxide to separate the unreacted 5-HOP and then with acidic water before it was dried over anhydrous sodium sulfate and

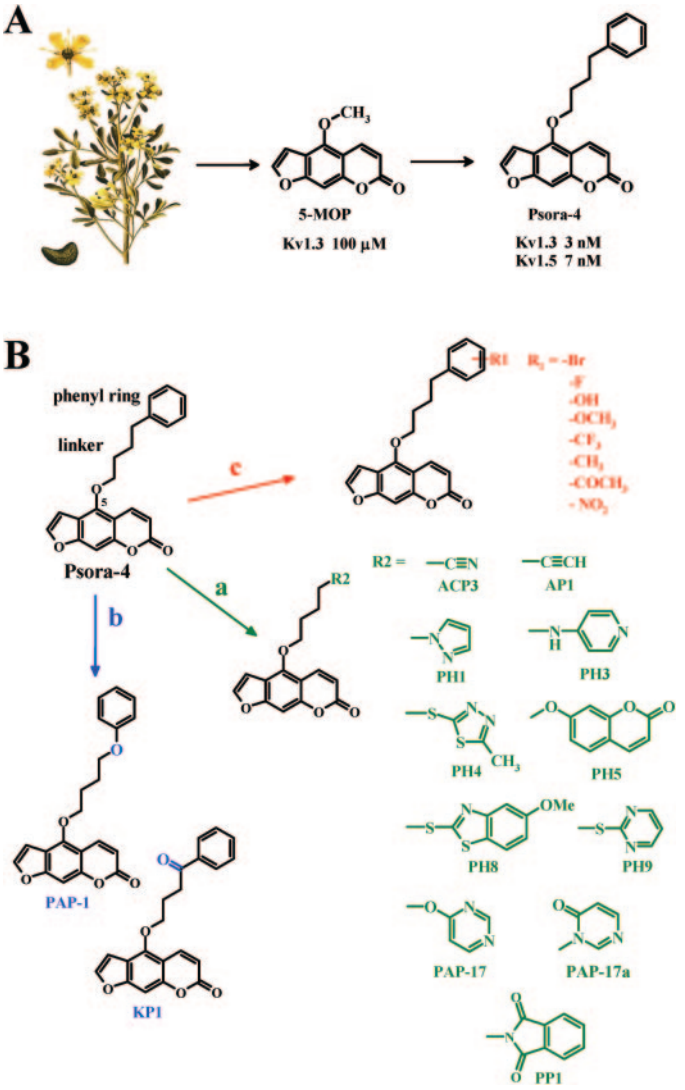

Fig. 1. A, *R. graveolens* was the source of 5-MOP, which served as a template for the Kv1.3 blocker Psora-4. B, design strategy for new Psora-4 analogs.

concentrated to dryness. The resulting residue was decolorized with charcoal and recrystallized.

General method B. 5-HOP was alkylated with 4-chloroiodobutane in dry acetone in the presence of an excess of potassium carbonate for 24 to 28 h at 25°C. After completion of the reaction, the product, 5-(4-chlorobutoxy)psoralen, was isolated according to general method A and then reacted with mercapto-, amino-, and hydroxy-substituted heteroaromatics or with substituted phenols to obtain the heteroaromatic and phenoxy-substituted compounds shown in Figs. 1B and 2.

General method C. To obtain phenoxy-substituted alkyl halides as reactants for general method A, elemental sodium was stirred in 120 ml of dry ethyl alcohol, and an equivalent amount of the phenol component was added drop-wise. After addition of an excess of 1,4-dibromobutane, the reaction mixture was refluxed for 4 h. The solvent was evaporated, and the residue was dissolved in 6% sodium hydroxide solution and extracted with ether. The organic layer was dried over sodium sulfate and evaporated to obtain the crude product.

All newly synthesized compounds were characterized by melting point, ^{1}H and ^{13}C NMR, mass spectrometry, and combustion analysis. ^{13}C data are given only for PAP-1, PAP-17, and PAP-17a, where it was necessary to determine the structure of the two reaction products. It is available upon request for other compounds.

5-(4-Chlorobutoxy)psoralen. 5-HOP (817 mg, 4.0 mmol), 4-chlorobutyl iodide (1.4 g, 6.4 mmol) and potassium carbonate (3.0 g) were stirred at 25°C in 80 ml of acetone for 30 h. After completion of the reaction, the acetone was evaporated and the resulting residue suspended in petroleum ether, filtered to separate the excess 4-chlorobutyl iodide, and dried under suction (1.10 g, 92.9%): m.p. = 115.6°C; ^{1}H-NMR (500 MHz, $CDCl_3$): δ [ppm] = 8.15 (d, 1H, ^3J = 9.8 Hz, 3-H), 7.60 (d, 1H, ^3J = 2.6 Hz, 5′-H), 7.17 (s, 1H, 8-H), 6.95 (d, 1H, ^3J = 2.2 Hz, 4′-H), 6.29 (d, 1H, ^3J = 9.8 Hz, 4-H), 4.52 (t, 2H, ^3J = 5.5 Hz, 5-OC$\underline{H}_2$CH$_2$CH $_2$CH$_2$Cl), 3.68 (t, 2H, ^3J = 5.8 Hz, 5-OCH$_2$CH$_2$CH$_2$C$\underline{H}_2$Cl), 2.08 (p, 4H, ^3J = 3.0 Hz, 5-OCH$_2$C$\underline{H}_2$C$\underline{H}_2$CH$_2$Cl).

5-(3-Cyanopropoxy)psoralen (ACP-3). 5-HOP (800 mg, 3.9 mmol), 4-chlorobutyronitrile (655.5 mg, 6.3 mmol) and potassium carbonate (2.6 g) were refluxed in 50 ml of 2-butanone for 48 h. The crude product was recrystallized from methanol (710 mg, 66.7%): m.p. = 155.2°C; ^{1}H NMR (500 MHz, $CDCl_3$): δ [ppm] = 8.13 (d, 1H, ^3J = 9.8 Hz, 3-H), 7.63 (d, 1H, ^3J = 2.0 Hz, 5′-H), 7.21 (s, 1H, 8-H), 6.98 (d, 1H, ^3J = 2.0 Hz, 4′-H), 6.32 (d, 1H, ^3J = 9.5 Hz, 4-H), 4.58 (t, 2H, ^3J = 5.8 Hz, 5-OC$\underline{H}_2$CH$_2$CH$_2$CN), 2.72 (t, 2H, ^3J = 5.7 Hz, 5-OCH$_2$CH$_2$C$\underline{H}_2$CN), 2.26 (p, 2H, ^3J = 6.3 Hz, 5-OCH$_2$C$\underline{H}_2$CH$_2$CN); MS (70 eV) *m/z*: 269 (100%, M$^+$), 202 (74%, [C$_{11}$H$_6$O$_4$]$^+$), 174 (63%, [202-CO]$^+$), 145 (26%), 118 (7%), 89 (14%); calculated for $C_{15}H_{11}NO_4$ (269.26): C, 66.91%; H, 4.12%; N, 5.01%; O, 23.77%. Found: C, 66.52%; H, 4.03%; N, 5.01%.

5-(4-Pentynyloxy)psoralen (AP-1). 5-HOP (500 mg, 2.4 mmol), 5-chloro-1-pentyne (405.8 mg, 3.9 mmol) and potassium carbonate (2.0 g) were refluxed in 30 ml of acetonitrile for 24 h. The crude product was recrystallized from methanol (55 mg, 8.3%): m.p. = 145.1°C: ^{1}H NMR (500 MHz, $CDCl_3$): δ [ppm] = 8.16 (d, 1H, ^3J = 9.8 Hz, 3-H), 7.60 (d, 1H, ^3J = 2.3 Hz, 5′-H), 7.17 (s, 1H, 8-H), 7.01 (d, 1H, ^3J = 1.5 Hz, 4′-H), 6.29 (d, 1H, ^3J = 9.8 Hz, 4-H), 4.56 (t, 2H, ^3J = 6.1 Hz, 5-OC$\underline{H}_2$CH$_2$CH$_2$C≡CH), 2.51 (q, 2H, ^3J = 2.6 Hz, 5-OCH$_2$CH$_2$C$\underline{H}_2$C≡CH), 2.09 (p, 2H, ^3J = 6.5 Hz, 5-OCH$_2$C$\underline{H}_2$CH$_2$C≡CH), 2.03 (t, 1H, ^4J = 2.6 Hz, 5-OCH$_2$CH$_2$CH$_2$C≡C$\underline{H}$); MS (70 eV) *m/z*: 268 (88%, M$^+$), 203 (15%), 202 (100%, [C$_{11}$H$_6$O$_4$]$^+$), 175 (8%), 174 (11%, [202-CO]$^+$), 173 (14%), 146 (7%), 145 (21%), 118 (8%), 89 (10%), 67 (5%, C_5H_7); calculated for $C_{16}H_{12}O_4$ (268.27): C, 71.64%; H, 4.51%; O, 23.86%. Found: C, 71.25%; H, 4.38%; LogP, 2.88.

5-[4-(1-*N*-Pyrazolyl)butoxy]psoralen (PH-1). 5-HOP (500 mg, 2.4 mmol), 4-iodo-1-chlorobutane (893 mg, 4.1 mmol) and potassium carbonate (2.0 g) were stirred at 25°C in 30 ml of acetone for 28 h. After completion of the reaction, the solvent was evaporated and the resulting residue refluxed for 50 h with pyrazole (400 mg, 5.9 mmol) and potassium carbonate (2.0 g) in 30 ml of 2-butanone. The crude product was recrystallized from an ethyl acetate/petroleum ether mixture (20:80) to yield white crystals (108 mg, 13.5%): m.p. = 145.6°C; ^{1}H NMR (500 MHz, DMSO-d_6): δ [ppm] = 8.17 (d, 1H, ^3J = 9.1 Hz, 3-H), 8.02 (s, 1H, 5′-H), 7.74 (s, 1H, 5-OCH$_2$CH$_2$CH$_2$CH$_2$C$_3$-$\underline{H}_3$N$_2$), 7.43 (s, 1H, 5-OCH$_2$CH$_2$CH$_2$CH$_2$C$_3$$\underline{H}_3N_2$), 7.34 (s, 1H, 8-H), 7.29 (s, 1H, 4′-H), 6.32 (d, 1H, ^3J = 9.1 Hz, 4-H), 4.47 (s, 2H, 5-OC-$\underline{H}_2$CH$_2$CH$_2$CH$_2$C$_3$H$_3$N$_2$), 4.20 (s, 2H, 5-OCH$_2$CH$_2$CH$_2$C$\underline{H}_2$C$_3$H$_3$N$_2$), 2.0 (s, 4H, 5-OCH$_2$C$\underline{H}_2$C$\underline{H}_2$CH$_2$C$_3$H$_3$N$_2$), 1.75 (s, 2H, 5-OCH$_2$CH$_2$C-$\underline{H}_2$CH$_2$C$_3$H$_3$N$_2$); MS (70 eV) *m/z*: 324 (29%, M$^+$), 202 (6%, [C$_{11}$H$_6$O-$_4$]$^+$), 174 (6%, [202-CO]$^+$), 123 (99%), 81 (26%), 69 (13%); calculated for $C_{18}H_{16}N_2O_4$(324.34): C, 66.66%; H, 4.97%; N, 8.64%; O, 19.73%. Found: C, 66.53%; H, 4.96%; N, 8.56%; LogP, 2.42.

5-[4-*N*-(4-Pyridinyl)aminobutoxy]psoralen (PH-3). 5-(4-Chlorobutoxy)psoralen (390 mg, 1.3 mmol) and 4-aminopyridine (628 mg, 6.7 mmol) were refluxed in 20 ml of acetonitrile for 45 h. The crude product was recrystallized from 2% acidic acetone (172 mg, 30.4%): m.p. = 133.9°C; ^{1}H NMR (500 MHz, DMSO-d_6): δ [ppm] = 8.27 (s, 1H, 5-OCH$_2$CH$_2$CH$_2$CH$_2$N$\underline{H}$C$_5$H$_4$N), 8.25 (d, 2H, ^3J = 7.41 Hz, 5-OCH$_2$CH$_2$CH$_2$CH$_2$NHC$_5$$\underline{H}_4$N), 8.18 (d, 1H, ^3J = 9.8 Hz, 3-H), 8.05 (d, 1H, ^3J = 2.6 Hz, 5′-H), 7.36 (s, 1H, 8-H), 7.33 (d, 1H, ^3J = 2.3 Hz, 4′-H), 6.85 (d, 2H, ^3J = 7.3 Hz, 5-OCH$_2$CH$_2$CH $_2$CH$_2$NHC$_5$$\underline{H}_4$N), 6.32 (d, 1H, ^3J = 9.8 Hz, 4-H), 4.52 (t, 2H, ^3J = 6.1 Hz, 5-OC$\underline{H}_2$CH$_2$CH-$_2$CH$_2$NHC$_5$H$_4$N), 4.22 (t, 2H, ^3J = 7.0 Hz, 5-OCH$_2$CH$_2$CH$_2$C$\underline{H}_2$NH-C$_5$H$_4$N), 1.99 (p, 2H, 5-OCH$_2$C$\underline{H}_2$CH$_2$CH$_2$NHC$_5$H$_4$N), 1.77 (p, 2H, 5-OCH$_2$CH$_2$C$\underline{H}_2$CH$_2$NHC$_5$H$_4$N); MS (70 eV) *m/z*: 350 (12%, M$^+$), 202 (99%, [C$_{11}$H$_6$O$_4$]$^+$), 174 (60%, [202-CO]$^+$), 184 (20%), 145 (11%), 123 (15%), 107 (46%), 94 (7%, $C_5H_6N_2$); calculated for $C_{20}H_{18}N_2O_4$ as dihydrochloride salt (423.38): C, 56.68%; H, 4.72%; N, 6.61%; O, 18.27%. Found: C, 56.69%; H, 4.84%; N, 6.58%; LogP, 1.79.

5-[4-(5-Methyl-1,3,4-thiadiazol-2-thiolyl)butoxy]psoralen (PH-4). 5-(4-Chlorobutoxy)psoralen (500 mg, 1.7 mmol), 2-mercapto-1,3,4-thiadiazole (361 mg, 2.7 mmol) and potassium carbonate (2.0 g) were refluxed in 30 ml of 2-butanone for 66 h. The oily residue was recrystallized from a petroleum ether/ethyl acetate (80:20) mixture (107 mg, 16.13%): m.p. = 92.1°C; ^{1}H NMR (500 MHz, $CDCl_3$): δ [ppm] = 8.15 (d, 1H, ^3J = 9.8 Hz, 3-H), 7.59 (d, 1H, ^3J = 2.5 Hz, 5′-H), 7.16 (s, 1H, 8-H), 6.95 (d, 1H, ^3J = 2.5 Hz, 4′-H), 6.29 (d, 1H, ^3J = 9.8 Hz, 4-H), 4.51 (t, 2H, ^3J = 5.8 Hz, 5-OC$\underline{H}_2$CH$_2$CH$_2$CH$_2$S-), 3.43 (t, 2H, ^3J = 6.9 Hz, 5-OCH$_2$CH$_2$CH$_2$C$\underline{H}_2$S-), 2.74 (s, 3H, 5″-CH$_3$), 2.09 (m, 4H, ^3J = 3.0 Hz, 5-OCH$_2$C$\underline{H}_2$C$\underline{H}_2$CH$_2$S-); MS (70 eV) *m/z*: 388 (62%, M$^+$), 202 (14%, [C$_{11}$H$_6$O$_4$]$^+$), 187 (96%, $C_7H_{11}N_2S_2$), 174 (12%, [202-CO]$^+$), 145 (10%), 133 (32%), 99 (34%, $C_3H_3N_2S$), 87 (8%, C_4H_7S), 55 (28%, C_4H_7); calculated for $C_{18}H_{16}N_2O_4S_2$ (388.47): C, 55.65%, H, 4.15%; N, 7.21%; O, 16.47%; S, 16.51%. Found: C, 55.44%; H, 4.15%; N, 7.39%; S, 16.77%; LogP, 2.85.

5-[4-(7-Coumarinyloxy)butoxy]psoralen (PH-5). 5-(4-Chlorobutoxy)psoralen (500 mg, 1.7 mmol), 7-hydroxycoumarin (443 mg, 2.7 mmol) and potassium carbonate (2.0 g) were refluxed in 30 ml of 2-butanone for 68 h. The oily residue obtained was recrystallized from a methanol/acetone (70:30) mixture (134 mg, 18.8%): m.p. = 147°C; ^{1}H NMR (500 MHz, $CDCl_3$): δ [ppm] = 8.15 (d, 1H, ^3J = 9.8 Hz, 3-H), 7.64 (d, 1H, ^3J = 9.5 Hz, 5-OCH$_2$CH$_2$CH$_2$CH$_2$OC$_9$$\underline{H}_5O_2$), 7.61 (d, 1H, ^3J = 2.1 Hz, 5′-H), 7.36 (dd, 1H, ^3J = 8.6 Hz, ^5J = 2.5 Hz, 5-OCH$_2$CH$_2$CH$_2$CH$_2$OC$_9$$\underline{H}_5O_2$), 7.16 (s, 1H, 8-H), 6.99 (d, 1H, ^3J = 2.1 Hz, 4′-H), 6.83 (m, 2H, 5-OCH$_2$CH$_2$CH$_2$CH$_2$OC$_9$$\underline{H}_5O_2$), 6.26 (d, 1H, ^3J = 9.5 Hz, 4-H), 6.20 (d, 1H, ^3J = 9.8 Hz, 5-OCH$_2$CH$_2$CH$_2$C-$\underline{H}_2$OC$_9$$\underline{H}_5O_2$), 4.57 (t, 2H, ^3J = 5.4 Hz, 5-OC$\underline{H}_2$CH$_2$CH$_2$CH$_2$OC$_9$H$_5$-O$_2$), 4.15 (t, 2H, ^3J = 5.0 Hz, 5-OCH$_2$CH$_2$CH$_2$C$\underline{H}_2$OC$_9$H$_5$O$_2$), 2.11 (m, 4H, ^3J = 2.6 Hz, 5-OCH$_2$C$\underline{H}_2$C$\underline{H}_2$CH$_2$OC$_9$H$_5$O$_2$); MS (70 eV) *m/z*: 418 (34%, M$^+$), 378 (68%), 217 (89%), 202 (20%, [C$_{11}$H$_6$O$_4$]$^+$), 175 (100%), 174 (14%, [202-CO]$^+$), 187 (16%), 145 (32%), 134 (26%), 89 (30%), 55 (48%, C_4H_7); calculated for $C_{24}H_{18}O_7$ (418.41) C, 68.90%; H, 4.34%; O, 26.77%. Found: C, 69.08%, H, 4.46%; LogP, 3.34.

5-[4-(5-Methoxy-1,3-benzothiazol-2-thiolyl)butoxy]psoralen (PH-8). 2-Mercapto-5-methoxy-1,3-benzothiazole (539 mg, 2.7 mmol) and potassium hydroxide (161 mg, 2.8 mmol) were refluxed in 25 ml

Strategy a:

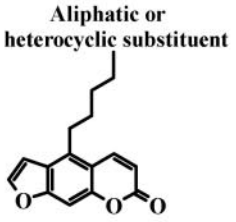

	EC_{50} Kv1.3	EC_{50} Kv1.5
ACP-3	1.3 μM	5 μM
AP-1	280 nM	500 nM
PH-1	450 nM	5 μM
PH-3	5 μM	5 μM
PH-4	175 nM	5 μM
PH-5	125 nM	5 μM
PH-8	35 nM	100 nM
PH-9	50 nM	159 nM
PAP-17	125 nM	425 nM
PAP-17a	7 μM	>5 μM
PP-1	450 nM	900 nM

Strategy b:

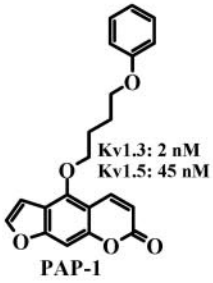

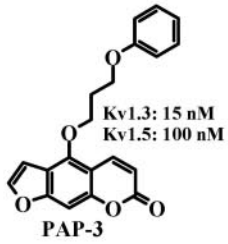

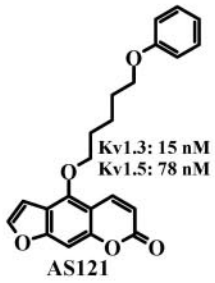

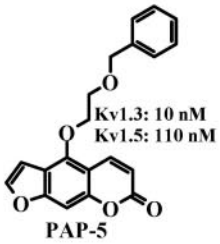

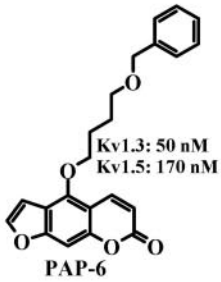

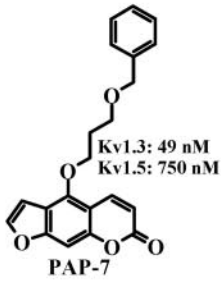

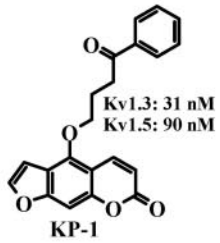

Strategy b + c:

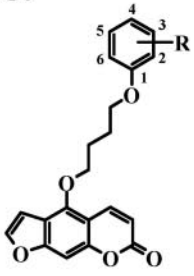

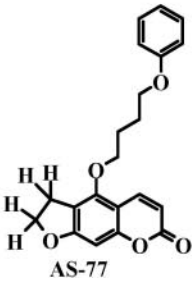

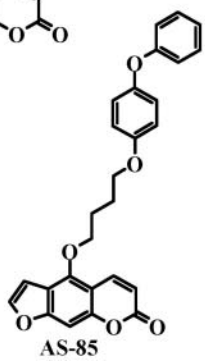

	R	EC_{50} Kv1.3	EC_{50} Kv1.5
AS-67	4-OCH_3	8 nM	10 nM
AS-68	3-OCH_3	18 nM	45 nM
AS-69	3,5-$(OCH_3)_2$	120 nM	150 nM
AS-96	4-CH_3	7 nM	20 nM
AS-118	3-CF_3	65 nM	250 nM
AS-111	4-F	12 nM	12 nM
AS-84	4-Cl	5 nM	10 nM
AS-78	4-NO_2	5 nM	105 nM
PAP-12	2-NO_2	61 nM	244 nM
PAP-13	3-NO_2	81 nM	90 nM
PAP-14	2,4-$(NO_2)_2$	140 nM	297 nM
PAP-10	2-OCH_3, 4-NO_2	500 nM	476 nM
PAP-11	2-NO_2, 4-CH_3	700 nM	248 nM
AS-85		16 nM	750 nM
AS-77		22 nM	45 nM

Fig. 2. Top, EC_{50} values of compounds synthesized under strategy a (see Fig. 1B for chemical structures). Middle, chemical structures and EC_{50} values of compounds from strategy b. Bottom, EC_{50} values and structures of compounds that were synthesized through a combination of strategies b + c. All compounds were tested three to five times at four to six concentrations and EC_{50} values were determined by fitting the Hill equation to the reduction of area under the current curve at 40 mV. The standard deviations were smaller than 10% in each case.

of methanol until the solution was clear. The solution was then concentrated to dryness under vacuum to obtain the dry potassium salt. To this potassium salt was added 20 ml of anhydrous acetonitrile, 5-(4-chlorobutoxy)psoralen (500 mg, 1.7 mmol), and sodium iodide (333 mg, 2.2 mmol), and the resulting mixture was refluxed for 69 h. The oily residue was recrystallized from a petroleum ether/acetone (80:20) mixture (600 mg, 48.8%): m.p. = 134.8°C; ^{1}H NMR (500 MHz, $CDCl_3$): δ [ppm] = 8.09 (d, 1H, ^3J = 9.8 Hz, 3-H), 7.61 (d, 1H, ^3J = 8.9 Hz, benzothiazole), 7.58 (d, 1H, ^3J = 2.3 Hz, 5′-H), 7.35 (d, 1H, ^4J = 2.2 Hz, benzothiazole), 7.14 (s, 1H, 8-H), 6.97 (dd, 1H, ^3J = 8.9 Hz, ^4J = 2.1 Hz, benzothiazole), 6.95 (d, 1H, ^3J = 2.8 Hz, 4′-H), 6.18 (d, 1H, ^3J = 9.8 Hz, 4-H), 4.53 (t, 2H, ^3J = 5.8 Hz, 5-OC$\underline{H}_2$CH$_2$CH$_2$CH$_2$S-), 3.87 (s, 3H, O-C$\underline{H}_3$), 3.48 (t, 2H, ^3J = 6.6 Hz, 5-OCH$_2$CH$_2$CH$_2$C$\underline{H}_2$S-), 2.11 (m, 4H, 5-OCH$_2$C$\underline{H}_2$C$\underline{H}_2$CH$_2$S-); MS (70 eV) *m/z*: 455 (6%, M^+), 453 (44%), 328 (28%), 252 (100%, $C_{12}H_{14}NOS_2$), 201 (6%), 196 (12%, $C_8H_6NOS_2$), 174 (14%, $[202\text{-}CO]^{+)}$, 145 (8%), 89 (6%), 55 (28%, C_4H_7); calculated for $C_{23}H_{19}NO_5S_2$ (455.56): C, 60.70%; H, 4.65%; N, 3.07%; O, 17.64%; S, 14.08%. Found: C, 60.70%; H, 4.59%; N, 3.09%; S, 13.94%; LogP, 4.36.

5-[4-(Pyrimidin-2-thiolyl)butoxy]psoralen (PH-9). 2-Mercaptopyrimidine (306 mg, 2.7 mmol) and potassium hydroxide (163 mg, 2.8 mmol) were refluxed in 50 ml of methanol until the solution was clear. The solution was then concentrated to dryness under reduced pressure to obtain the potassium salt. To the potassium salt was added acetonitrile (30 ml), 5-(4-chlorobutoxy)psoralen (500 mg, 1.7 mmol), and sodium iodide (333 mg, 2.2 mmol), and the mixture was refluxed for 67 h. The oily residue was recrystallized from methanol (244 mg, 38.78%): m.p. = 107.1°C; ^{1}H NMR (500 MHz, $CDCl_3$): δ [ppm] = 8.51 (d, 2H, pyrimidine), 8.14 (d, 1H, ^3J = 10.1 Hz, 3-H), 7.59 (d, 1H, ^3J = 2.4 Hz, 5′-H), 7.16 (s, 1H, 8-H), 7.0 (t, 1H, ^3J = 4.9 Hz, pyrimidine), 6.96 (d, 1H, ^3J = 1.5 Hz, 4′-H), 6.25 (d, 1H, ^3J = 9.8 Hz, 4-H), 4.52 (t, 2H, ^3J = 5.8 Hz, 5-OC$\underline{H}_2$CH$_2$CH$_2$CH$_2$S-), 3.29 (t, 2H, ^3J = 6.8 Hz, 5-OCH$_2$CH$_2$CH$_2$C$\underline{H}_2$S-), 2.01 (m, 4H, 5-OCH$_2$C$\underline{H}_2$C$\underline{H}_2$CH$_2$S-); MS (70 eV) *m/z*: 368 (27%, M^+), 202 (8%, $[C_{11}H_6O_4]^+$), 167 (100%, $C_8H_{11}N_2S$), 125 (34%), 113 (37%), 55 (26%, C_4H_7); calculated for $C_{19}H_{16}N_2O_4S$ (368.41): C, 61.94%; H, 4.38%; N, 7.60%; O, 17.37%; S, 8.70%. Found: C, 61.85%; H, 4.34%; N, 7.41%; S, 8.66%; LogP, 3.00.

5-[4-(*N*-Phthalimido)butoxy]psoralen (PP-1). 5-HOP (500 mg, 2.5 mmol), *N*-(4-bromobutyl)phthalimide (1.12 g, 3.9 mmol), and potassium carbonate (2.2 g) were refluxed in 50 ml of acetonitrile for 72 h. The crude solid was recrystallized from methanol (260 mg, 26.1%): m.p. = 177.9°C; ^{1}H NMR (500 MHz, $CDCl_3$): δ [ppm] = 8.14 (d, 1H, ^3J = 9.8 Hz, 3-H), 7.8 (dd, 4H, ^3J = 5.4 Hz, ^4J = 3.0 Hz, 5-OCH$_2$CH$_2$CH$_2$CH$_2$NC$_8\underline{H}_4$O$_2$), 7.6 (d, 1H, ^3J = 2.4 Hz, 5′-H), 7.13 (s, 1H, 8-H), 6.95 (d, 1H, ^3J = 1.6 Hz, 4′-H), 6.30 (d, 1H, ^3J = 9.8 Hz, 4-H), 4.5 (t, 2H, ^3J = 5.7 Hz, 5-OC$\underline{H}_2$CH$_2$CH$_2$CH$_2$NC$_8$H$_4$O$_2$), 3.82 (t, 2H, ^3J = 6.6 Hz, 5-OCH$_2$CH$_2$CH$_2$C$\underline{H}_2$NC$_8$H$_4$O$_2$), 1.98 (p, 4H, ^3J = 3.2 Hz, 5-OCH$_2$C$\underline{H}_2$C$\underline{H}_2$CH$_2$NC$_8$H$_4$O$_2$); MS (70 eV) *m/z*: 403 (13%, M^+), 202 (72%, $[C_{11}H_6O_4]^+$), 174 (8%, $[202\text{-}CO]^+$), 160 (99%), 148 (6%), 130 (14%), 55 (5%, C_4H_7); calculated for $C_{23}H_{17}NO_6$ (403.40): C, 68.48%; H, 4.25%; N, 3.47%; O, 23.80%. Found: C 68.17%; H, 4.32%; N, 3.36%; LogP, 3.21.

5-(4-Pyrimidynyloxybutoxy)psoralen (PAP-17). 5-(4-Chlorobutoxy)psoralen (500 mg, 1.7 mmol), sodium iodide (512 mg, 3.4 mmol), 4-hydroxypyrimidine (263 mg, 3.4 mmol), and potassium carbonate (3.0 g) were refluxed in 30 ml of acetonitrile for 90 h. The crude product mixture was separated by column chromatography on silica gel (60–200 mesh, 50 g) by gradient elution using a petroleum ether/ethyl acetate mixture and yielded PAP-17 and PAP-17a. PAP-17 (99.6 mg, 19.92%, m.p. = 126.4°C) was formed by *O*-alkylation of 4-hydroxypyrimidine: ^{1}H NMR (500 MHz, $CDCl_3$): δ [ppm] = 8.80 (s, 1H, 2″-H), 8.47 (d, 1H, ^3J = 9.0 Hz, 6″-H), 8.17 (d, 1H, ^3J = 9.7 Hz, 3-H), 7.60 (d, 1H, ^3J = 2.2 Hz, 5′-H), 7.17 (s, 1H, 8-H), 6.96 (d, 1H, ^3J = 1.8 Hz, 4′-H), 6.74 (d, 1H, ^3J = 5.4 Hz, 5″-H) 6.30 (d, 1H, ^3J = 9.7 Hz, 4-H), 4.54 (t, 2H, ^3J = 5.3 Hz, 5-OC$\underline{H}_2$CH$_2$CH$_2$CH$_2$O-C$_4$H$_3$N$_2$), 4.50 (t, 2H, ^3J = 5.1 Hz, 5-OCH$_2$CH$_2$CH$_2$C$\underline{H}_2$OC$_4$H$_3$N$_2$), 2.2 (m, 4H, 5-OCH$_2$C$\underline{H}_2$C$\underline{H}_2$CH$_2$OC$_4$H$_3$N$_2$); ^{13}C-NMR (DMSO-d_6, 75 MHz): δ [ppm] = 25.38 and 26.68 (5-OCH$_2$(*C*H$_2$)$_2$CH$_2$OC$_4$H$_3$N$_2$); 65.90 and 72.29 (5-O*C*H$_2$(CH$_2$)$_2$*C*H$_2$OC$_4$H$_3$N$_2$); 93.97 (C-8); 105.01 (C-4′); 106.66 (C-4a); 112.61 (C-3 and C-5″); 113.18 (C-6); 139.16 (C-4); 144.84 (C-5′); 148.74 (C-5); 152.63 (C-8a); 156.98 (C-6″); 158.20 (C-2″) 158.34 (C-7); 161.15 (C-2); 168.83 (C-4″). MS (70 eV) *m/z*: 352 (24%, M^+), 202 (58%, $[C_{11}H_6O_4]^+$), 174 (29%, $[202\text{-}CO]^+$), 151 (100%, $C_8H_{11}N_2O$), 145 (12%, $[174\text{-}CO]^+$), 109 (8%, $[C_6H_5O_2]^+$), 97 (60%); molecular weight calculated for $C_{19}H_{16}N_2O_5$, 352.10592; found by high-resolution mass spectrometry, 352.10596.

5-[4-(4-Oxopyrimidin-3-yl)butoxy]psoralen (PAP-17a). PAP-17a was formed as a side product during the synthesis of PAP-17. During the alkylation reaction, 4-hydroxypyrimidine tautomerises to 4-oxopyrimidine which through *N*-alkylation formed PAP-17a (248 mg, 49.5%, m.*p* = 178.1°C): ^{1}H NMR (500 MHz, $CDCl_3$): δ [ppm] = 8.21 (s, 1H, 6″-H), 8.13 (d, 1H, ^3J = 10.1 Hz, 3-H), 7.91 (d, 1H, ^3J = 6.3 Hz, 3″-H), 7.60 (d, 1H, ^3J = 1.7 Hz, 5′-H), 7.17 (s, 1H, 8-H), 6.94 (d, 1H, ^3J = 2.6 Hz, 4′-H), 6.48 (d, ^3J = 6.1 Hz, 4″-H), 6.29 (d, 1H, ^3J = 9.9 Hz, 4-H), 4.49 (t, 2H, ^3J = 6.0 Hz, 5-OC$\underline{H}_2$CH$_2$CH$_2$CH$_2$O-C$_4$H$_3$N$_2$), 4.06 (t, 2H, ^3J = 7.35 Hz, 5-OCH$_2$CH$_2$CH$_2$C$\underline{H}_2$OC$_4$H$_3$N$_2$), 2.2 (m, 4H, 5-OCH$_2$C$\underline{H}_2$C$\underline{H}_2$CH$_2$OC$_4$H$_3$N$_2$); ^{13}C-NMR (DMSO-d_6, 75 MHz): δ [ppm] = 26.01 and 27.06 (5-O-CH$_2$(*C*H$_2$)$_2$CH$_2$OC$_4$H$_3$N$_2$); 46.92 and 72.01 (5-O*C*H$_2$(CH$_2$)$_2$*C*H$_2$OC$_4$H$_3$N$_2$); 94.28 (C-8); 104.88 (C-4′); 106.81 (C-4a); 112.87 (C-3); 113.44 (C-6); 116.16 (C-3″); 139.03 (C-4); 145.03 (C-5′); 148.50 (C-5); 151.02 (C-4″); 152.63 (C-8a); 153.11 (C-6″) 158.17 (C-7); 160.82 (C-2″); 161.11 (C-2). MS (70 eV) *m/z*: 352 (13%, M^+), 202 (12%, $[C_{11}H_6O_4]^+$), 174 (10%, $[202\text{-}CO]^+$), 151 (100%, $C_8H_{11}N_2O$), 145 (5%, $[174\text{-}CO]^+$), 109 (6%, $[C_6H_5O_2]^+$), 97 (27%); molecular weight calculated for $C_{19}H_{16}N_2O_5$, 352.1059; found by high-resolution mass spectrometry, 352.1066.

5-(4-Phenoxybutoxy)psoralen (PAP-1). 5-HOP (700 mg, 3.5 mmol), 4-phenoxybutyl bromide (600 mg, 3.5 mmol), and potassium carbonate (2.0 g) were refluxed in 30 ml of 2-butanone for 24 h. The crude product was recrystallized from methanol-acetone (80:20) as a white solid (734 mg, 60.5%): m.p. = 104°C; ^{1}H NMR (500 MHz, $CDCl_3$): δ [ppm] = 8.13 (d, 1H, ^3J = 9.7 Hz, 3-H), 7.59 (d, 1H, ^3J = 2.0 Hz, 5′-H), 7.30 (m, 5H, 5-OCH$_2$CH$_2$CH$_2$CH$_2$OC$_6\underline{H}_5$), 7.15 (s, 1H, 8-H), 6.91 (d, 1H, ^3J = 2.0 Hz, 4′-H), 6.25 (d, 1H, ^3J = 9.8 Hz, 4-H), 4.56 (t, 2H, ^3J = 6.14 Hz, 5-OC$\underline{H}_2$CH$_2$CH$_2$CH$_2$OC$_6$H$_5$), 4.09 (t, 2H, ^3J = 5.80 Hz, 5-OCH$_2$CH$_2$CH$_2$C$\underline{H}_2$OC$_6$H$_5$), 2.09 (m, 4H, ^3J = 4.21 Hz, 5-OCH$_2$C$\underline{H}_2$C$\underline{H}_2$CH$_2$OC$_6$H$_5$); ^{13}C-NMR (DMSO-d_6, 75 MHz): δ [ppm] = 25.26 and 26.18 (5-O-CH$_2$(*C*H$_2$)$_2$CH$_2$OC$_6$H$_5$); 66.91 and 72.29 (5-O*C*H$_2$(CH$_2$)$_2$*C*H$_2$OC$_6$H$_5$); 93.18 (C-8); 105.62 (C-4′); 105.98 (C-4a); 112.29 (C-3); 112.92 (C-6); 114.39 (C-3″ and C-5″); 120.39 (C-4″); 129.41 (C-2″ and C-6″); 139.44 (C-4); 145.89 (C-5′); 148.72 (C-5); 152.11 (C-8a); 157.63 (C-1″); 158.48 (C-7); 160.07 (C-2); MS (70 eV) *m/z*: 350 (20%, M^+), 202 (9%, $[C_{11}H_6O_4]^+$), 201 (5%), 174 (13%, $[202\text{-}CO]^+$), 173 (4%), 150 (11%), 149 (100%), 145 (8%), 107 (100%, $[149\text{-}C_3H_6]^+$), 94 (9%, C_6H_6O), 89 (4%), 77 (37%, C_6H_5), 65 (6%, C_5H_5); calculated for $C_{21}H_{18}O_5$ (350.37): C, 71.99%; H, 5.18%; O, 22.83%. Found: C,71.92%; H, 5.08%; LogP, 4.03.

5-(3-Phenoxypropoxy)psoralen (PAP-3). 5-HOP (700 mg, 3.5 mmol), 3-phenoxypropyl bromide (750 mg, 3.5 mmol), and potassium carbonate (3.0 g) were refluxed in 30 ml of 2-butanone for 36 h. The oily residue was recrystallized from methanol/ethyl acetate (10:90) as a white solid (390 mg, 33.5%): m.p. = 108.4°C; ^{1}H NMR (500 MHz, $CDCl_3$): δ [ppm] = 8.13 (d, 1H, ^3J = 9.8 Hz, 3-H), 7.59 (d, 1H, ^3J = 2.3 Hz, 5′-H), 7.31 (t, 3H, 3″-H, 4″-H, 5″-H), 7.16 (s, 1H, 8-H), 6.99 (d, 1H, ^3J = 2.4 Hz, 4′-H), 6.93 (d, 2H, 2″-H, 6″-H), 6.24 (d, 1H, ^3J = 9.5 Hz, 4-H), 4.66 (t, 2H, ^3J = 5.9 Hz, 5-OC$\underline{H}_2$CH$_2$CH$_2$OC$_6$H$_5$), 4.26 (t, 2H, ^3J = 6.0 Hz, 5-OCH$_2$CH$_2$C$\underline{H}_2$OC$_6$H$_5$), 2.38 (p, 2H, ^3J = 6.0 Hz, 5-OCH$_2$C$\underline{H}_2$CH$_2$OC$_6$H$_5$); MS (70 eV) *m/z*: 336 (91%, M^+), 203 (7%), 202 (57%, $[C_{11}H_6O_4]^+$), 201 (11%), 174 (16%, $[202\text{-}CO]^+$), 173 (11%), 145 (14%), 135 (90%), 134 (9%), 108 (8%), 107 (100%), 95 (8%), 89 (9%), 77 (62%, C_6H_5), 65 (9%, C_5H_5); calculated for $C_{21}H_{18}O_5$ (336.35): C, 71.42%; H, 4.79%; O, 23.78%. Found: C, 71.09%, H, 4.74%. LogP: 3.76.

5-(2-Benzyloxyethoxy)psoralen (PAP-5). 5-HOP (600 mg, 2.9 mmol), benzyl-2-bromoethyl ether (1.0 g, 4.6 mmol), and potassium

carbonate (2.0 g) were refluxed in 30 ml of 2-butanone for 16 h. The oily residue was recrystallized from 70% methanol to obtain a white solid (123 mg, 12.3%): m.p. = 90.9°C; ^{1}H NMR (500 MHz, $CDCl_3$): δ [ppm] = 8.19 (d, 1H, ^3J = 9.7 Hz, 3-H), 7.59 (d, 1H, ^3J = 2.2 Hz, 5′-H), 7.37 (m, 5H, 5-$OCH_2CH_2OCH_2C_6H_5$), 7.19 (s, 1H, 8-H), 6.95 (d, 1H, ^3J = 2.0 Hz, 4′-H), 6.25 (d, 1H, ^3J = 9.7 Hz, 4-H), 4.64 (s, 2H, 5-$OCH_2CH_2OCH_2C_6H_5$), 4.58 (t, 2H, ^3J = 4.62 Hz, 5-$OCH_2CH_2OCH_2C_6H_5$), 3.88 (t, 2H, ^3J = 4.56 Hz, 5-$OCH_2CH_2OCH_2C_6H_5$); MS (70 eV) *m/z*: 336 (35%, M^+), 105 (5%), 91 (100%, $[C_7H_7]^+$); calculated for $C_{20}H_{16}O_5$ (336.35): C, 71.42%; H, 4.79%; O, 23.78%. Found: C, 70.65%; H, 4.73%; LogP, 3.34.

5-(5-Phenoxypentoxy)psoralen (AS-121). 1-Bromo-5-phenoxypentane was synthesized according to general method C using 1,5-dibromopentane instead of 1,4-dibromobutane. 5-HOP (300 mg, 1.5 mmol), 1-bromo-5-phenoxypentane (600 mg, 2.6 mmol), and potassium carbonate (2.0 g) were then refluxed in 30 ml of acetone for 24 h. The crude product was recrystallized from methanol/water (80:20) as a white solid (232 mg, 42.4%): m.p. = 91°C; ^{1}H NMR (300 MHz, DMSO-d_6): δ [ppm] = 8.19 (d, 1H, ^3J = 9.7 Hz, 4-H), 8.02 (s, 1H, 5′-H), 7.25 to 7.33 (m, 4H, 8-H, 4′-H and 5-$OCH_2CH_2CH_2CH_2CH_2OC_6H_5$), 6.90 to 6.93 (m, 3H, 5-$OCH_2CH_2CH_2CH_2CH_2OC_6H_5$), 6.30 (d, 1H, ^3J = 9.7 Hz, 3-H), 4.52 (t, 2H, ^3J = 6.0 Hz, 5-$OCH_2CH_2CH_2CH_2CH_2CH_2OC_6H_5$), 4.00 (t, 2H, ^3J = 6.2 Hz, 5-$OCH_2CH_2CH_2CH_2CH_2OC_6H_5$), 1.77 to 1.93 (m, 4H, 5-$OCH_2CH_2CH_2CH_2CH_2OC_6H_5$), 1.63 to 1.71 (m, 2H, 5-$OCH_2CH_2CH_2CH_2CH_2OC_6H_5$); MS (70 eV) *m/z*: 364 M^+ (9%, M^+), 202 (22%, $[C_{11}H_6O_4]^+$), 163 (44%, $[C_{11}H_{15}O]^+$), 107 (40%, $[C_6H_5O\text{-}CH_2]^+$), 69 (100%, $[C_5H_9]^+$), 41 (52%, $[C_3H_5]^+$); calculated for $C_{22}H_{20}O_5$ (364.40): C, 72.51%; H, 5.53%; O, 21.96%. Found: C, 72.74%; H, 5.68%; LogP, 4.40.

5-(4-Benzyloxybutoxy)psoralen (PAP-6). 5-HOP (700 mg, 3.5 mmol), benzyl-4-bromobutyl ether (850 mg, 3.5 mmol), and potassium carbonate (2.0 g) were refluxed in 30 ml of 2-butanone for 24 h. The oily residue was recrystallized from 80% methanol (171 mg, 13.4%): m.p. = 78.4°C; ^{1}H NMR (500 MHz, $CDCl_3$): δ [ppm] = 8.14 (d, 1H, ^3J = 9.8 Hz, 3-H), 7.55 (d, 1H, ^3J = 2.5 Hz, 5′-H), 7.34 (m, 5H, 5-$OCH_2CH_2CH_2CH_2OCH_2C_6H_5$), 7.13 (s, 1H, 8-H), 6.91 (d, 1H, ^3J = 2.4 Hz, 4′-H), 6.25 (d, 1H, ^3J = 9.8 Hz, 4-H), 4.54 (s, 2H, 5-$OCH_2CH_2CH_2CH_2OCH_2C_6H_5$), 4.49 (t, 2H, ^3J = 6.5 Hz, 5-$OCH_2CH_2CH_2CH_2OCH_2C_6H_5$), 3.59 (t, 2H, ^3J = 6.1 Hz, 5-$OCH_2CH_2CH_2CH_2OCH_2C_6H_5$), 2.00 (p, 2H, ^3J = 6.9 Hz, 5-$OCH_2CH_2CH_2CH_2OCH_2C_6H_5$), 1.87 (p, 2H, ^3J = 6.8 Hz, 5-$OCH_2CH_2CH_2CH_2OCH_2C_6H_5$); MS (70 eV) *m/z*: 364 (37%, M^+), 292 (10%), 202 (7%, $[C_{11}H_6O_4]^+$), 174 (6%, [202-CO]$^+$), 163 (12%), 91 (100%, C_7H_7), 71 (8%); calculated for $C_{22}H_{20}O_5$ (364.40): C, 72.51%; H, 5.53%; O, 21.95%. Found: C, 72.36%; H, 5.46%; LogP, 4.02.

5-(3-Benzyloxypropoxy)psoralen (PAP-7). 5-HOP (1.0 g, 4.9 mmol), benzyl-3-bromopropyl ether (1.36 g, 5.9 mmol), and potassium carbonate (3.4 g) were refluxed in 30 ml of 2-butanone for 24 h. The oily residue was recrystallized from 70% methanol (700 mg, 40.4%): m.p. = 75.2°C; ^{1}H NMR (500 MHz, $CDCl_3$): δ [ppm] = 8.06 (d, 1H, ^3J = 9.7 Hz, 3-H), 7.57 (d, 1H, ^3J = 2.2 Hz, 5′-H), 7.29 (m, 5H, ^3J = 6.3 Hz, 5-$OCH_2CH_2CH_2OCH_2C_6H_5$), 7.15 (s, 1H, 8-H), 6.98 (d, 1H, ^3J = 2.2 Hz, 4′-H), 6.21 (d, 1H, ^3J = 9.8 Hz, 4-H), 4.58 (t, 2H, ^3J = 6.1 Hz, 5-$OCH_2CH_2CH_2OCH_2C_6H_5$), 4.55 (s, 2H, 5-$OCH_2CH_2CH_2OCH_2C_6H_5$), 3.73 (t, 2H, ^3J = 5.7 Hz, 5-$OCH_2CH_2CH_2OCH_2C_6H_5$), 2.18 (p, 2H, ^3J = 6.1 Hz, 5-$OCH_2CH_2CH_2OCH_2C_6H_5$); MS (70 eV) *m/z*: 350 (25%, M^+), 202 (9%, $[C_{11}H_6O_4]^+$), 174 (5%, [202-CO]$^+$), 91 (100%, $[C_7H_7]^+$); calculated for $C_{21}H_{18}O_5$(350.37): C, 71.99%; H, 5.18%; O, 22.83%. Found: C, 71.64%; H, 5.34%; LogP, 3.66.

5-(4-Phenyl-3-oxobutoxy)psoralen (KP-1). 4-Chlorobutyrophenone (497 mg, 2.7 mmol) and sodium iodide (445 mg, 2.9 mmol) were refluxed in 30 ml of acetone for 1.5 h to obtain the iodo derivative. To this slurry were added 5-HOP (500 mg, 2.5 mmol), potassium carbonate (2.0 g), and the resulting mixture was then refluxed for 140 h. The solid residue was recrystallized from a petroleum ether/acetone (90:10) mixture (295 mg, 34.3%): m.p. = 129.1°C; ^{1}H NMR (500 MHz, $CDCl_3$): δ [ppm] = 8.13 (d, 1H, ^3J = 9.9 Hz, 3-H), 8.01 (d, 2H, ^3J = 7.9 Hz, ^4J = 0.95 Hz, 2″-H, 6″-H), 7.62 (t, 1H, ^3J = 7.4 Hz, 3″-H, 5″-H), 7.60 (d, 1H, ^3J = 2.4 Hz, 5′-H), 7.50 (t, 2H, ^3J = 7.7 Hz, 4″-H), 7.15 (s, 1H, 8-H), 6.99 (d, 1H, ^3J = 2.5 Hz, 4′-H), 6.26 (d, 1H, ^3J = 9.8 Hz, 4-H) 4.59 (t, 2H, ^3J = 6.2 Hz, 5-$OCH_2CH_2CH_2COC_6H_5$), 3.28 (t, 2H, ^3J = 6.8 Hz, 5-$OCH_2CH_2CH_2COC_6H_5$), 2.38 (p, 2H, ^3J = 6.5 Hz, 5-$OCH_2CH_2CH_2COC_6H_5$); MS (70 eV) *m/z*: 348 (34%, M^+), 202 (5%, $[C_{11}H_6O_4]^+$), 147(99%, $C_{10}H_{10}O$), 174, (5%, [202-CO]$^+$), 105 (71%, C_3H_6), 77 (33%, C_6H_5); calculated for $C_{21}H_{16}O_5$ (348.36): C, 72.41%; H, 4.63%; O, 22.96%. Found: C, 72.18%; H, 4.75%; LogP, 3.31.

5-[4-(4-Methoxyphenoxy)butoxy]psoralen (AS-67). 5-HOP (300 mg, 1.5 mmol), 1-bromo-4-(4-methoxyphenoxy)butane (600 mg, 2.5 mmol, obtained by general method C), and potassium carbonate (2.0 g) were refluxed in 30 ml of acetone for 24 h. The crude product was recrystallized from methanol-water (80:20) as a white solid (201 mg, 35.2%): m.p. = 111.5°C; ^{1}H NMR (300 MHz, DMSO-d_6): δ [ppm] = 8.18 (d, 1H, ^3J = 9.8 Hz, 4-H), 8.03 (d, 1H, ^3J = 2.3 Hz, 5′-H), 7.32 to 7.34 (m, 2H, 8-H and 4′-H), 6.81 to 6.87 (m, 4H, 5-$OCH_2(CH_2)_2CH_2OC_6H_4OCH_3$), 6.81 to 6.87 (m, 4H, 5-$OCH_2(CH_2)_2CH_2OC_6H_4OCH_3$), 6.30 (d, 1H, ^3J = 9.8 Hz, 3-H), 4.57 (t, 2H, ^3J = 5.7 Hz, 5-$OCH_2(CH_2)_2CH_2OC_6H_4OCH_3$), 4.00 (t, 2H, ^3J = 5.8 Hz, 5-$OCH_2(CH_2)_2CH_2OC_6H_4OCH_3$), 3.69 (s, 3H, -$OCH_3$), 1.91 to 1.99 (m, 4H, 5-$OCH_2(CH_2)_2CH_2OC_6H_4OCH_3$); MS (70 eV) *m/z*: 380 (14%, M^+), 257 (8%), 215 (7%), 202 (5%, $[C_{11}H_6O_4]^+$), 179 (69%, $[C_{11}H_{15}O_2]^+$), 145 (6%), 137 (100%, $[CH_3OC_6H_4OCH_2]^+$), 109 (29%), 107 (18%, $[C_6H_5OCH_2]^+$), 77 (23%, $[C_6H_5]^+$), 55 (61%, $[C_4H_7]^+$), 41 (15%, $[C_3H_5]^+$); calculated for $C_{22}H_{20}O_6$ (380.4): C, 69.46%; H, 5.30%; O, 25.24%. Found: C, 69.52%; H, 5.39%; LogP, 3.89.

5-[4-(3-Methoxyphenoxy)butoxy]psoralen (AS-68). 5-HOP (300 mg, 1.5 mmol), 1-bromo-4-(3-methoxyphenoxy)butane (600 mg, 2.5 mmol, obtained by general method C), and potassium carbonate (2.0 g) were refluxed in 30 ml of acetone for 24 h. The crude product was recrystallized from methanol-water (80:20) as a white solid (178 mg, 31.2%): m.p. = 102.5°C; ^{1}H NMR (300 MHz, DMSO-d_6): δ [ppm] = 8.18 (d, 1H, ^3J = 9.8 Hz, 4-H), 8.02 (d, 1H, ^3J = 1.9 Hz, 5″-H), 7.33 (s, 2H, 8-H and 4′-H), 7.15 (t, 1H, ^3J = 8.14 Hz, 8-H), 6.45 to 6.51 (m, 3H, 2″-H, 4″-H and 6″-H), 6.29 (d, 1H, ^3J = 9.8 Hz, 3-H), 4.58 (t, 2H, ^3J = 5.4 Hz, 5-$OCH_2(CH_2)_2CH_2OC_6H_4OCH_3$), 4.05 (t, 2H, ^3J = 5.4 Hz, 5-O-$CH_2(CH_2)_2CH_2OC_6H_4OCH_3$), 3.71 (s, 3H, -$OCH_3$), 1.91 to 1.99 (m, 4H, 5-$OCH_2(CH_2)_2CH_2OC_6H_4OCH_3$); MS (70 eV) *m/z*: 380 (14%, M^+), 257 (8%), 202 (5%, $[C_{11}H_6O_4]^+$), 179 (84%, $[C_{11}H_{15}O_2]^+$), 145 (6%), 137 (100%, $[CH_3OC_6H_4OCH_2]^+$), 109 (14%), 107 (32%, $[C_6H_5OCH_2]^+$), 77 (27%, $[C_6H_5]^+$), 55 (63%, $[C_4H_7]^+$), 41 (12%, $[C_3H_5]^+$); calculated for $C_{22}H_{20}O_6$ (380.4): C, 69.46%; H, 5.30; O, 25.24%. Found: C, 69.89%; H, 5.38%; LogP, 3.99.

5-[4-(3,5-Dimethoxyphenoxy)butoxy]psoralen (AS-69). 5-HOP (300 mg, 1.5 mmol), 1-bromo-4-(3,5-dimethoxyphenoxy)butane (700 mg, 2.6 mmol, obtained by general method C) and potassium carbonate (2.0 g) were refluxed in 30 ml of acetone for 24 h. The crude product was recrystallized from methanol/acetone (80:20) as a white solid (182 mg, 29.6%): m.p. = 139°C; ^{1}H NMR (300 MHz, DMSO-d_6): δ [ppm] = 8.19 (d, 1H, ^3J = 9.8 Hz, 4-H), 8.03 (d, 1H, ^3J = 2.1 Hz, 5′-H), 7.34 (s, 2H, 8-H and 4′-H), 6.31 (d, 1H, ^3J = 9.8 Hz, 3-H), 6.07 (s, 3H, 2″-H, 4″-H and 6″-H), 4.58 (t, 2H, ^3J = 5.4 Hz, 5-$OCH_2(CH_2)_2CH_2OC_6H_3(OCH_3)_2$), 4.05 (t, 2H, ^3J = 5.4 Hz, 5-$OCH_2(CH_2)_2CH_2OC_6H_3(OCH_3)_2$), 3.69 (s, 6H, -$(OCH_3)_2$), 1.93 to 1.97 (m, 4H, 5-$OCH_2(CH_2)_2CH_2OC_6H_3(OCH_3)_2$); MS (70 eV) *m/z*: 410 (12%, M^+), 209 (100%, $[C_{12}H_{17}O_3]^+$), 202 (5%, $[C_{11}H_6O_4]^+$), 167 (75%, $[(CH_3O)_2C_6H_3OCH_2]^+$), 137 (34%, $[CH_3OC_6H_4OCH_2]^+$), 122 (15%), 107 (10%, $[C_6H_5OCH_2]^+$), 77 (11%, $[C_6H_5]^+$), 55 (46%, $[C_4H_7]^+$), 41 (6%, $[C_3H_5]^+$); calculated for $C_{23}H_{22}O_7$ (410.43): C, 67.31%; H, 5.40%; O, 27.29%. Found: C, 66.92%; H, 5.60%; LogP, 3.94.

5-[4-(4-Nitrophenoxy)butoxy]psoralen (AS-78). 5-HOP (300 mg, 1.5 mmol), 1-bromo-4-(4-nitrophenoxy)butane (700 mg, 2.7 mmol, obtained by general method C), and potassium carbonate (2.0 g) were refluxed in 30 ml of acetone for 24 h. The crude product was recrystallized from methanol/acetone (80:20) as a yellow solid (291 mg, 49.1%): m.p. = 132°C; ^{1}H NMR (300 MHz, DMSO-d_6): δ [ppm] =

8.16 (d, 2H, ^3J = 9.1 Hz, 3″-H and 5″-H), 8.15 (d, 1H, ^3J = 9.6 Hz, 4-H), 8.00 (d, 1H, ^3J = 2.1 Hz, 5′-H), 7.30 (d, 1H, ^3J = 1.9 Hz, 4′-H), 7.28 (s, 1H, 8-H), 7.10 (d, 2H, ^3J = 9.2 Hz, 2″-H and 6″-H), 6.27 (d, 1H, ^3J = 9.8 Hz, 3-H), 4.56 (s, 2H, 5-OC$\underline{H}_2$(CH$_2$)$_2$CH$_2$OC$_6$H$_4$NO$_2$), 4.05 (s, 2H, 5-OCH$_2$(CH$_2$)$_2$C$\underline{H}_2$OC$_6$H$_4$NO$_2$), 1.99 (s, 4H, 5-OCH$_2$(C$\underline{H}_2$)$_2$CH$_2$OC$_6$H$_4$NO$_2$); MS (70 eV) *m/z*: 395 (12%, M$^+$), 202 (30%, [C$_{11}$H$_6$O$_4$]$^+$), 194 (100%, [C$_{10}$H$_{12}$O$_3$N]$^+$), 174 (26%, [202-CO]$^+$), 152 (82%, [O$_2$NC$_6$H$_4$OCH$_2$]$^+$), 133 (17%), 106 (17%), 89 (13%), 75 (12%), 55 (84%, [C$_4$H$_7$]$^+$), 41 (11%); calculated for C$_{21}$H$_{17}$O$_7$ (395.34): C, 63.80%; H, 4.33%; N, 3.54%; O, 28.33%. Found: C, 63.79%; H, 4.46%; N, 3.60%; LogP, 3.91.

5-[4-(4-Chlorphenoxy)butoxy]psoralen (AS-84). 5-HOP (300 mg, 1.5 mmol), 1-bromo-4-(4-chlorophenoxy)butane (700 mg, 2.8 mmol, obtained by General Method C), and potassium carbonate (2.0 g) were refluxed in 30 ml of acetone for 24 h. The crude product was recrystallized from methanol/water (80:20) as a white solid (247 mg, 42.8%): m.p. = 142.5°C; ^{1}H NMR (300 MHz, DMSO-d_6): δ [ppm] = 8.15 (d, 1H, ^3J = 9.8 Hz, 4-H), 8.01 (d, 1H, ^3J = 2.0 Hz, 5′-H), 7.31 (s, 2H, 8-H and 4′-H), 7.29 (d, 2H, ^3J = 8.9 Hz, 3″-H and 5″-H), 6.93 (d, 2H, ^3J = 8.9 Hz, 2″-H and 6″-H), 6.28 (d, 1H, ^3J = 9.8 Hz, 3-H), 4.55 (m, 2H, 5-OC$\underline{H}_2$(CH$_2$)$_2$CH$_2$OC$_6$H$_4$Cl), 4.05 (m, 2H, 5-OCH$_2$(CH$_2$)$_2$C$\underline{H}_2$OC$_6$H$_4$Cl), 1.95 to 1.96 (m, 4H, 5-OCH$_2$(C$\underline{H}_2$)$_2$CH$_2$OC$_6$H$_4$Cl); MS (70 eV) *m/z*: 384 (10%, M$^+$), 202 (14%, [C$_{11}$H$_6$O$_4$]$^+$), 183 (80%, [C$_{10}$H$_{12}$OCl]$^+$), 174 (11%, [202-CO]$^+$), 141 (100%, [ClC$_6$H$_4$OCH$_2$]$^+$), 113 (18%), 111 (23%), 89 (7%), 77 (9%, [C$_6$H$_5$]$^+$), 55 (72%, [C$_4$H$_7$]$^+$), 41 (5%); calculated for C$_{21}$H$_{17}$ClO$_5$ (384.82): C, 65.55%; H, 4.45%; Cl, 9.21%; O, 20.79%. Found: C, 65.23%; H, 4.57%; LogP, 4.50.

5-[4-(4-Phenoxyphenoxy)butoxy]psoralen (AS-85). 5-HOP (300 mg, 1.5 mmol), 1-bromo-4-(4-phenoxyphenoxy)butane (800 mg, 2.5 mmol, obtained by general method C), and potassium carbonate (2.0 g) were refluxed in 30 ml of acetone for 24 h. The crude product was recrystallized from ethanol/acetone (70:30) as a white solid (165 mg, 24.9%): m.p. = 137°C; ^{1}H NMR (300 MHz, DMSO-d_6): δ [ppm] = 8.17 (d, 1H, ^3J = 9.8 Hz, 4-H), 8.02 (s, 1H, 5′-H), 7.31 to 7.35 (m, 4H, 8-H, 4′-H and -O-C$_6\underline{H}_4$OC$_6\underline{H}_5$), 7.06 (t, 1H, 4‴-H), 6.89 to 6.96 (m, 6H, -OC$_6\underline{H}_4$OC$_6\underline{H}_5$), 6.29 (d, 1H, ^3J = 9.7 Hz, 3-H), 4.57 (s, 2H, 5-OC$\underline{H}$-$_2$(CH$_2$)$_2$CH$_2$OC$_6$H$_4$OC$_6$H$_5$), 4.05 (s, 2H, 5-OCH$_2$(CH$_2$)$_2$C$\underline{H}_2$OC$_6$H$_4$O-C$_6$H$_5$), 1.97 (s, 4H, 5-OCH$_2$(C$\underline{H}_2$)$_2$CH$_2$OC$_6$H$_4$OC$_6$H$_5$); MS (70 eV) *m/z*: 442 (25%, M$^+$), 257 (16%), 241 (100%, [C$_6$H$_5$OC$_{10}$H$_{12}$O]$^+$), 215 (12%), 199 (100%, [C$_6$H$_5$OC$_8$H$_8$O]$^+$), 186 (100%, [C$_6$H$_5$OC$_7$H$_5$O]$^+$), 171 (12%), 148 (38%), 129 (13%), 115 (17%), 93 (10%), 77 (49%, [C$_6$H$_5$]$^+$), 55 (70%, [C$_4$H$_7$]$^+$), 41 (7%); calculated for C$_{27}$H$_{22}$O$_6$ (442.47): C, 73.29%; H, 5.01%; O, 21.7%. Found: C, 73.24%; H, 5.09%; LogP, 5.03.

5-[4-(4-Methylphenoxy)butoxy]psoralen (AS-96). 5-HOP (300 mg, 1.5 mmol), 1-bromo-4-(4-methylphenoxy)butane (600 mg, 2.5 mmol, obtained by general method C), and potassium carbonate (2.0 g) were refluxed in 30 ml of acetone for 24 h. The crude product was recrystallized from methanol/acetone (80:20) as a white solid (253 mg, 46.3%): m.p. = 128°C; ^{1}H NMR (300 MHz, DMSO-d_6): δ [ppm] = 8.15 (d, 1H, ^3J = 9.8 Hz, 4-H), 8.02 (d, 1H, ^3J = 2.1 Hz, 5′-H), 7.31 (s, 2H, 8-H and 4′-H), 7.06 (d, 2H, ^3J = 8.4 Hz, 2″-H and 6″-H), 6.80 (d, 2H, ^3J = 8.5 Hz, 3″-H and 5″-H), 6.28 (d, 1H, ^3J = 9.8 Hz, 3-H), 4.56 (t, 2H, ^3J = 5.6 Hz, 5-OC$\underline{H}_2$(CH$_2$)$_2$CH$_2$OC$_6$H$_4$CH$_3$), 4.02 (t, 2H, ^3J = 5.7 Hz, 5-OCH$_2$(CH$_2$)$_2$C$\underline{H}_2$OC$_6$H$_4$CH$_3$), 2.22 (s, 3H, -CH$_3$), 1.92 to 2.01 (m, 4H, 5-OCH$_2$(C$\underline{H}_2$)$_2$CH$_2$OC$_6$H$_4$CH$_3$); MS (70 eV) *m/z*: 364 (10%, M$^+$), 202 (5%, [C$_{11}$H$_6$O$_4$]$^+$), 163 (87%, [C$_{11}$H$_{15}$O]$^+$), 121 (100%, [CH$_3$C$_6$H$_4$OCH$_2$]$^+$), 91 (33%, [C$_7$H$_7$]$^+$), 65 (9%), 55 (35%, [C$_4$H$_7$]$^+$), 41 (4%); calculated for C$_{22}$H$_{20}$O$_5$ (364.40): C, 72.51%; H, 5.53%; O, 21.96%. Found: C, 72.59%; H, 5.65%; LogP, 4.42.

5-[4-(4-Fluorphenoxy)butoxy]psoralen (AS-111). 5-HOP (300 mg, 1.5 mmol), 1-bromo-4-(4-fluorophenoxy)butane (600 mg, 2.5 mmol, obtained by general method C), and potassium carbonate (2.0 g) were refluxed in 30 ml of acetone for 24 h. The crude product was recrystallized from methanol/water (80:20) as a white solid (192 mg, 34.7%): m.p. = 121°C; ^{1}H NMR (300 MHz, DMSO-d_6): δ [ppm] = 8.14 (d, 1H, ^3J = 9.8 Hz, 4-H), 8.01 (d, 1H, ^3J = 2.0 Hz, 5′-H), 7.30 (s, 2H, 4′-H and 8-H), 6.89 to 6.94 (m, 2H, 5-OCH$_2$(CH$_2$)$_2$CH$_2$OC$_6\underline{H}_4$F), 6.27 (d, 1H, ^3J = 9.8 Hz, 3-H), 4.53 to 4.55 (m, 2H, 5-OC$\underline{H}_2$(CH$_2$)$_2$CH$_2$O-C$_6$H$_4$F), 4.01 to 4.05 (m, 2H, 5-OCH$_2$(CH$_2$)$_2$C$\underline{H}_2$OC$_6$H$_4$F), 1.94 to 1.96 (m, 4H, 5-OCH$_2$(C$\underline{H}_2$)$_2$CH$_2$OC$_6$H$_4$F); MS (70 eV) *m/z*: 368 (11%, M$^+$), 202 (11%, [C$_{11}$H$_6$O$_4$]$^+$), 174 (11%, [202-CO]$^+$), 167 (83%, [C$_{10}$H$_{12}$O-F]$^+$), 125 (100%, [FC$_6$H$_4$OCH$_2$]$^+$), 95 (23%), 89 (5%), 55 (46%, [C$_4$H$_7$]$^+$), 41 (3%); calculated for C$_{21}$H$_{17}$FO$_5$ (368.37): C, 68.47%; H, 4.65%; F, 5.16%; O, 21.72%. Found: C, 68.15%; H, 4.65; LogP, 4.11.

5-[4-(3-Trifluormethylphenoxy)butoxy]psoralen (AS-118). 5-HOP (300 mg, 1.5 mmol), 1-bromo-4-(3-trifluoromethylphenoxy)-butane (700 mg, 2.4 mmol, obtained by general method C), and potassium carbonate (2.0 g) were refluxed in 30 ml of acetone for 24 h. The crude product was recrystallized from methanol/acetone (60:40) as a white solid (142 mg, 22.6%): m.p. = 118°C; ^{1}H NMR (300 MHz, DMSO-d_6): δ [ppm] = 8.15 (d, 1H, ^3J = 9.8 Hz, 4-H), 8.01 (d, 1H, ^3J = 2.3 Hz, 5′-H), 7.49 (t, 1H, ^3J = 7.93 Hz, 5″-H), 7.18 to 7.32 (m, 5H, 2″-H, 4″-H, 6″-H, 8-H and 4′-H), 6.26 (d, 1H, ^3J = 9.8 Hz, 3-H), 4.57 (s, 2H, 5-OC$\underline{H}_2$(CH$_2$)$_2$CH$_2$OC$_6$H$_4$CF$_3$), 4.15 (s, 2H, 5-O-CH$_2$(CH$_2$)$_2$C$\underline{H}_2$OC$_6$H$_4$CF$_3$), 1.98 (s, 4H, 5-OCH$_2$(C$\underline{H}_2$)$_2$C-H$_2$OC$_6$H$_4$CF$_3$); MS (70 eV) *m/z*: 418 (14%, M$^+$), 217 (79%), 202 (19%, [C$_{11}$H$_6$O$_4$]$^+$), 175 (100%, [C$_{12}$H$_{15}$O]$^+$), 145 (37%), 127 (7%), 109 (14%), 89 (6%), 55 (75%, [C$_4$H$_7$]$^+$), 41 (4%); calculated for C$_{22}$H$_{17}$F$_3$O$_5$ (418.37): C, 63.16%; H, 4.10%; F, 13.62%; O, 19.12%. Found: C, 63.19%; H, 4.09%; LogP, 4.65.

5-(4-[2-Methoxy-4-nitrophenoxy]butoxy)psoralen (PAP-10). 5-(4-Chlorobutoxy)psoralen (500 mg, 1.7 mmol) and sodium iodide (741 mg, 4.9 mmol) were refluxed in 15 ml of anhydrous acetonitrile for 60 min to obtain the iodo derivative. To this solution were added 4-nitroguaicol (837 mg, 4.9 mmol), potassium carbonate (3.0 g), and 10 ml of acetonitrile, and the mixture was refluxed for 72 h. The solid residue was recrystallized from a methanol/acetone (80:20) mixture (382 mg, 52.6%): m.p. = 170.5°C; ^{1}H NMR (500 MHz, CDCl$_3$): δ [ppm] = 8.15 (d, 1H, ^3J = 9.8 Hz, 3-H), 7.91 (d, 1H, ^4J = 2.6 Hz, 3″-H), 7.75 (dd, 1H, ^3J = 2.7 Hz, 5″-H), 7.60 (d, 1H, ^3J = 2.2 Hz, 5′-H), 7.16 (s, 1H, 8-H), 6.98 (d, 1H, ^3J = 2.4 Hz, 4′-H), 6.93 (d, 1H, ^3J = 2.2 Hz, 6″-H), 6.26 (d, 1H, ^3J = 9.7 Hz, 4-H), 4.59 (t, 2H, ^3J = 6.0 Hz, 5-OC$\underline{H}_2$CH$_2$CH$_2$CH$_2$OC$_6$H$_3$), 4.23 (t, 2H, ^3J = 5.7 Hz, 5-OCH$_2$CH$_2$CH$_2$C$\underline{H}_2$OC$_6$H$_3$), 3.915 (s, 3H, 2″-OCH$_3$), 2.14 (m, 4H, 5-OCH$_2$C$\underline{H}_2$C$\underline{H}_2$CH$_2$OC$_6$H$_3$); MS (70 eV) *m/z*: 425 (24%, M$^+$), 395 (11%, [C$_{22}$H$_{19}$O$_7$]$^+$), 257 (12%), 224 (100%), 202 (44%, [C$_{11}$H$_6$O$_4$]$^+$), 182 (68%,), 174, (26%, [202-CO]$^+$), 145 (18%, [174-CO]$^+$); molecular weight calculated for C$_{22}$H$_{19}$NO$_8$, 425.1110; found by high-resolution mass spectrometry, 425.1112

5-(4-[4-Methyl-2-nitrophenoxy]butoxy)psoralen (PAP-11). 5-(4-Chlorobutoxy)psoralen (500 mg, 1.7 mmol) and sodium iodide (741 mg, 4.9 mmol) were refluxed in 15 ml of acetonitrile for 60 min to obtain the iodo derivative. To this solution were added 2-nitro-p-cresol (523 mg, 3.4 mmol), potassium carbonate (4.0 g), and 10 ml of acetonitrile. The mixture was refluxed for 69 h. The solid residue was recrystallized from a methanol/acetone (80:20) mixture (447 mg, 64.0%): m.p. = 124.5°C; ^{1}H NMR (500 MHz, CDCl$_3$): δ [ppm] = 8.14 (d, 1H, ^3J = 9.7 Hz, 3-H), 7.63 (d, 1H, ^4J = 1.8 Hz, 3″-H), 7.59 (d, 1H, ^3J = 2.4 Hz, 5′-H), 7.31 (d, 1H, ^3J = 8.2 Hz, 5″-H), 7.14 (s, 1H, 8-H), 6.98 (d, 1H, ^3J = 2.5 Hz, 4′-H), 6.96 (d, 1H, ^3J = 8.76 Hz, 6″-H), 6.26 (d, 1H, ^3J = 9.8 Hz, 4-H), 4.56 (t, 2H, ^3J = 5.7 Hz, 5-OC$\underline{H}_2$CH$_2$CH-$_2$CH$_2$OC$_6$H$_3$), 4.17 (t, 2H, ^3J = 6.0 Hz, 5-OCH$_2$CH$_2$CH$_2$C$\underline{H}_2$OC$_6$H$_3$), 2.34 (s, 3H, 4″-CH$_3$), 2.05 (m, 4H, ^3J = 4.216 Hz, 5-OCH$_2$C$\underline{H}_2$C$\underline{H}_2$C-H$_2$OC$_6$H$_3$); MS (70 eV) *m/z*: 409 (22%, M$^+$), 379 (20%, [C$_{22}$H$_{19}$O$_6$]$^+$), 257 (90%), 224 (100%), 202 (86%, [C$_{11}$H$_6$O$_4$]$^+$), 174, (52%, [202-CO]$^+$), 145 (30%, [174-CO]$^+$); molecular weight calculated for C$_{22}$H$_{19}$NO$_7$, 409.1161; found by high-resolution mass spectrometry, 409.1170

5-(4-[2-Nitrophenoxy]butoxy)psoralen (PAP-12). 5-(4-Chlorobutoxy)psoralen (500 mg, 1.7 mmol) and sodium iodide (512 mg, 3.4 mmol) were refluxed in 15 ml of acetonitrile for 1 h to obtain the iodo derivative. To this solution were added 2-nitrophenol (475 mg, 3.4 mmol), potassium carbonate (4.0 g), and 15 ml of acetonitrile. The mixture was refluxed for 29 h. The solid residue was recrystallized from a methanol/acetone (80:20) mixture (380 mg, 56.3%): m.p. =

121.8°C; ^{1}H NMR (500 MHz, $CDCl_3$): δ [ppm] = 8.14 (d, 1H, ^3J = 9.7 Hz, 3-H), 7.82 to 7.86 (overlapping dd, 2H, ^4J = 1.6 Hz, ^3J = 8.3 Hz, ^3J = 7.9 Hz, 3″-H, 6″-H), 7.60 (d, 1H, ^3J = 2.5 Hz, 5′-H), 7.52 to 7.55 (t, 2H, ^3J = 7.6 Hz, ^4J = 1.0 Hz, 3″-H, 4″-H), 7.15 (s, 1H, 8-H), 6.99 (d, 1H, ^3J = 2.4 Hz, 4′-H), 6.26 (d, 1H, ^3J = 9.7 Hz, 4-H), 4.57 (t, 2H, ^3J = 5.8 Hz, 5-OC$\underline{H}_2$CH$_2$CH$_2$CH$_2$OC$_6$H$_4$), 4.23 (t, 2H, ^3J = 2.8 Hz, 5-OCH$_2$CH$_2$CH$_2$C$\underline{H}_2$OC$_6$H$_4$), 2.09 to 2.16 (m, 4H, 5-OCH$_2$C$\underline{H}_2$C$\underline{H}_2$-CH$_2$OC$_6$H$_4$); MS (70 eV) *m/z*: 395 (36%, M^+), 365 (14%, [M-30]$^+$), 332 (78%), 283 (8%), 202 (9%, [$C_{11}H_6O_4$]$^+$), 194 (60%, [$C_{10}H_{12}NO_3$]$^+$), 122 (48%), 109 (8%), 92 (10%); molecular weight calculated for $C_{21}H_{20}O_5$, 395.10050; found by high-resolution mass spectrometry, 395.10053.

5-(4-[3-Nitrophenoxy]butoxy)psoralen (PAP-13). 5-(4-Chlorobutoxy)psoralen (500 mg, 1.7 mmol) and sodium iodide (512 mg, 3.4 mmol) were refluxed in 15 ml of acetonitrile for 1 h to obtain the iodo derivative. To this solution were added 3-nitrophenol (475 mg, 3.4 mmol), potassium carbonate (4.0 g), and 15 ml of acetonitrile, and the mixture was refluxed for 29 h. The solid residue was recrystallized from a methanol/acetone (80:20) mixture (286 mg, 42.4%): m.p. = 140.3°C; ^{1}H NMR (500 MHz, $CDCl_3$): δ [ppm] = 8.15 (d, 1H, ^3J = 9.7 Hz, 3-H), 7.84 (dd, 1H, ^3J = 8.1 Hz, ^4J = 1.6 Hz, 4″-H), 7.61 (d, 1H, ^3J = 2.3 Hz, 5′-H), 7.42 (t, 1H, ^3J = 8.3 Hz, 5″-H), 7.41 (t, 1H, ^4J = 2.2 Hz, 2″-H), 7.22 (dd, 1H, ^3J = 8.1 Hz, ^4J = 2.3 Hz, 6″-H) 7.16 (s, 1H, 8-H), 6.97 (d, 1H, ^3J = 2.2 Hz, 4′-H), 6.27 (d, 1H, ^3J = 9.8 Hz, 4-H), 4.56 (t, 2H, ^3J = 5.8 Hz, 5-OC$\underline{H}_2$CH$_2$CH$_2$CH$_2$OC$_6$H$_4$), 4.16 (t, 2H, ^3J = 5.6 Hz, 5-OCH$_2$CH$_2$CH$_2$C$\underline{H}_2$OC$_6$H$_4$), 2.12 (m, 4H, 5-OCH$_2$C$\underline{H}_2$C$\underline{H}_2$CH$_2$OC$_6$H$_4$); MS (70 eV) *m/z*: 395 (32%, M^+), 365 (14%, [M-30]$^+$), 292 (56%), 202 (100%, [$C_{11}H_6O_4$]$^+$), 194 (28%, [$C_{10}H_{12}NO_3$]$^+$), 174 (48%, [202-CO]$^+$), 145 (16%, [174-CO]$^+$), 109 (8%, [$C_6H_5O_2$]$^+$), 93 (14%, C_6H_5O); molecular weight calculated for $C_{21}H_{17}NO_7$, 395.10050; found by high-resolution mass spectrometry, 395.10103.

5-(4-[2,4-Dinitrophenoxy]butoxy)psoralen (PAP-14). 5-(4-Chlorobutoxy)psoralen (500 mg, 1.7 mmol), sodium iodide (512 mg, 3.4 mmol), 2,4-dinitrophenol (629 mg, 3.4 mmol), and potassium carbonate (3.0 g) were refluxed in 30 ml of acetonitrile for 50 h. The solid residue was recrystallized from a methanol/acetone (80:20) mixture (82 mg, 11.0%): m.p. = 134.2°C; ^{1}H NMR (500 MHz, $CDCl_3$): δ [ppm] = 8.78 (d, 1H, ^4J = 2.8 Hz, 3″-H), 8.45 (dd, 1H, ^3J = 9.0 Hz, ^4J = 2.8 Hz, 5″-H), 8.15 (d, 1H, ^3J = 9.7 Hz, 3-H), 7.61 (d, 1H, ^3J = 2.0 Hz, 5′-H), 7.22 (d, 1H, ^3J = 9.5 Hz, 6″-H), 7.17 (s, 1H, 8-H), 6.98 (d, 1H, ^3J = 2.1 Hz, 4′-H), 6.29 (d, 1H, ^3J = 9.8 Hz, 4-H), 4.57 (t, 2H, ^3J = 5.3 Hz, 5-OC$\underline{H}_2$CH$_2$CH$_2$CH$_2$OC$_6$H$_3$), 4.36 (t, 2H, ^3J = 5.1 Hz, 5-OCH$_2$CH$_2$CH$_2$C$\underline{H}_2$OC$_6$H$_3$), 2.2 (m, 4H, 5-OCH$_2$C$\underline{H}_2$C$\underline{H}_2$CH$_2$OC$_6$H$_3$); MS (70 eV) *m/z*: 440 (44%, M^+), 384 (18%, M^+-[$C_2H_2{}^+$NO]), 283 (16%), 202 (100%, [$C_{11}H_6O_4$]$^+$), 174 (34%, [202-CO]$^+$), 145 (12%, [174-CO]$^+$); molecular weight calculated for $C_{21}H_{16}N_2O_9$, 440.08558; found by high-resolution mass spectrometry, 440.08598.

5-(4-Phenoxybutoxy)-4′,5′-dihydropsoralen (AS-77). PAP-1 (175 mg, 0.5 mmol) was dissolved in 40 ml of ethanol. After addition of 80 mg of 10% palladium on carbon, it was agitated in a hydration bomb for 5 h under 2.1 bar of pressure. The Pd/C was then filtered off, the solution evaporated, and the remaining residue was purified by medium-pressure lipid chromatography with cyclohexane/ethyl acetate (80:20). Yield: (110 mg, 62.9%); m.p. = 93°C; ^{1}H NMR (300 MHz, DMSO-d_6): δ [ppm] = 7.99 (d, 1H, ^3J = 9.7 Hz, H-4), 7.25 to 7.30 (m, 2H, 5-OCH$_2$(CH$_2$)$_2$CH$_2$OC$_6$H$\underline{5}$), 6.90 to 6.94 (m, 3H, 5-O-CH$_2$(CH$_2$)$_2$CH$_2$-O-C$_6$H$\underline{5}$), 6.13 (d, 1H, ^3J = 9.7 Hz, H-3), 6.53 (s, 1H, H-8), 4.63 (t, 2H, ^3J = 8.5 Hz, H-5′), 4.31 (s, 2H, 5-OC$\underline{H}_2$(CH$_2$)$_2$CH$_2$OC$_6$H$_5$), 4.05 (s, 2H, 5-OCH$_2$(CH$_2$)$_2$C$\underline{H}_2$OC$_6$H$_5$), 3.42 (t, 2H, ^3J = 8.5 Hz, H-4′), 1.91 (s, 4H, 5-OCH$_2$(C$\underline{H}_2$)$_2$CH$_2$OC$_6$H$_5$); MS (70 eV) *m/z*: 352 (18%, M^+), 204 (4%, [$C_{11}H_8O_4$]$^+$), 176 (6%, [204-CO]$^+$), 149 (65%, [$C_{10}H_{13}O$]$^+$), 107 (100%, [$C_6H_5OCH_2$]$^+$), 95 (5%), 77 (28%, [C_6H_5]$^+$), 55 (25%, [C_4H_7]$^+$); molecular weight calculated for $C_{21}H_{20}O_5$, 352.13107; found by high-resolution mass spectrometry, 352.13091.

LogP Values. LogP (log of octanol-water partition coefficient, a measure of the hydrophobicity) values of compounds were determined by high-performance liquid chromatography with a binary high-performance liquid chromatography pump (Waters 1525; Waters, Milford, MA), a Kromasil 100 C18 column (5 μM, 60 × 4.6 mm; EKA Chemical Separation Products, Bohus, Sweden), and a Waters 2475 multiwavelength fluorescence detector. Compounds were eluted with a gradient changing from 30% acetonitrile and 70% Sørensen's phosphate buffer, 11 mM, pH 7.4, to 78% acetonitrile and 22% buffer over 70 min. 4-Methylbenzaldehyde, toluene, ethyl-, *n*-propyl-, *n*-butyl-, *n*-pentyl-, *n*-hexyl-, *n*-heptyl, and *n*-octylbenzene were used as standards.

Cells, Cell Lines, and Clones. Throughout the article, we are using the new IUPHAR nomenclature for ion channels (Gutman et al., 2003). Cells stably expressing *mKv1.1*, *rKv1.2*, *mKv1.3*, *hKv1.5*, and *mKv3.1* have been described previously (Grissmer et al., 1994). Cell lines stably expressing other mammalian ion channels were gifts from several sources: *mKv1.7* in CHL cells and *hKCa2.3* in COS-7 cells (Aurora Biosciences Corp., San Diego, CA); *hKv1.4* and *rKv4.2* in LTK cells (Michael Tamkun, University of Colorado, Boulder, CO); *hKv2.1* in HEK293 cells (James Trimmer, University of California Davis, Davis, CA); *Kv11.1* (HERG) in HEK293 cells (Craig January, University of Wisconsin, Madison, WI); *hKCa1.1, rKCa2.1* and *hKCa3.1* in HEK-293 cells (Khaled Houamed, University of Chicago, Chicago, IL); *hNav1.4* in HEK-293 cells (Frank Lehmann-Horn, University of Ulm, Germany); and *Cav1.2* in HEK-293 cells (Franz Hofmann, Munich, Germany). RBL-2H3 (expressing *Kir2.1*) and N1E-115 neuroblastoma cells (expressing *Nav1.2*) were obtained from the American Type Culture Collection (Manassas, VA). *hKv1.6* and *rKv3.2* (both in pcDNA3) were obtained from Protinac GmbH (Hamburg, Germany) and transiently-transfected into COS-7 cells with Fugene-6 (Roche) according to the manufacturer's protocol. The *hKv1.3*-H399T and A413C mutants were a generous gift from Tobias Dreker and Stephan Grissmer (University of Ulm, Germany), whereas the H399Y and A413V (Panyi et al., 1995) mutants were kindly supplied by Carol Deutsch (University of Pennsylvania, Philadelphia, PA).

Electrophysiology. All compounds used for electrophysiological testing were >98% pure as determined by combustion analysis. All experiments were conducted in the whole-cell configuration of the patch-clamp technique with a holding potential of −80 mV unless otherwise stated. Pipette resistances averaged 2.0 MΩ, and series resistance compensation of 80% was employed when currents exceeded 2 nA. Kv1.3 currents were elicited by repeated 200-ms or 2-s pulses from −80 to 40 mV, applied at intervals of 30 or 60 s. Kv1.3 currents were recorded in normal Ringer solution with a Ca^{2+}-free pipette solution containing 145 mM KF, 10 mM HEPES, 10 mM EGTA, 2 mM $MgCl_2$, pH 7.2, 300 mOsM. EC_{50} values and Hill coefficients were determined by fitting the Hill equation to the reduction of area under the current curve measured at 40 mV. Kv1.1, Kv1.5, Kv1.4, Kv1.6, Kv1.7, Kv2.1, Kv3.1, Kv3.2, and Kv4.2 currents were recorded with 200-ms depolarizing pulses to 40 mV applied every 10 s (Grissmer et al., 1994; Wulff et al., 2000; Bardien-Kruger et al., 2002). For Kv1.2, we applied 200-ms pulses to 40 mV every 5 s to allow for the channel's use-dependent activation (Grissmer et al., 1994). HERG (Kv11.1) currents were recorded with a 2-step pulse from −80 mV first to 20 mV for 2 s and then to −50 mV for 2 s (Zhou et al., 1998) and the reduction of both peak and tail current by the drug was determined.

The inward rectifier (*rKir2.1*) in RBL cells was studied with ramp pulses from −150 to 0 mV applied every 10 s and a Na^+ aspartate Ringer external and a K^+ aspartate-based pipette solution containing 50 nM free Ca^{2+}. For measurements of IK_{Ca} (*KCa3.1*) SK_{Ca} (*KCa2.3*), and BK_{Ca} (*KCa1.1*) currents, we used an internal pipette solution containing 145 mM K^+ aspartate, 2 mM $MgCl_2$, 10 mM HEPES, 10 mM K_2EGTA, and 8.5 mM $CaCl_2$ (1 μM free Ca^{2+}), pH 7.2, 290 to 310 mOsM, and an external solution containing 160 mM Na^+ aspartate, 4.5 mM KCl, 2 mM $CaCl_2$, 1 mM $MgCl_2$, and 5 mM HEPES, pH 7.4, 290 to 310 mOsM. BK_{Ca} currents were elicited by 200-ms voltage ramps from −80 to 80 mV applied every 10 s, and channel block was measured as a reduction of slope conductance at 35 mV. IK_{Ca} and SK_{Ca} currents were elicited by 200-ms voltage

ramps from −120 mV to 40 mV applied every 10 s, and the reduction of slope conductance at −80 mV by drug was taken as a measure of channel block (Wulff et al., 2000). Nav1.2 currents from N1E-115 cells and Nav1.4 currents from stably transfected HEK cells were recorded with 100-ms pulses from −80 to 0 mV every 10 s with a KCl-based pipette solution and normal Ringer's solution as an external solution. Cav1.2 currents were elicited by 600-ms depolarizing pulses from −80 to 20 mV every 10 s with a CsCl-based pipette solution and an external solution containing 30 mM $BaCl_2$ (Kolski-Andreaco et al., 2004). Blockade of both Na^+ and Ca^{2+} currents was determined as reduction of the current minimum. Swelling-activated chloride currents were elicited from activated human T cells with a hyperosmolar cesium glutamate-based pipette solution (420 mOsM) and ramp pulses from −120 to 60 mV every 10 s (Ross et al., 1994).

Cytotoxicity Assays. Jurkat E61 and MEL cells were seeded at 5×10^5 cells/ml in 12-well plates. Compounds were added at concentrations of 10 nM, 100 nM, and 10 μM in a final DMSO concentration of 0.1%, which was found not to affect cell viability. After 48 h, the cells in each well were well mixed and resuspended, and the number of trypan blue-positive cells in three aliquots from each well was determined under a light microscope. The test was repeated twice.

Ames Test. The mutagenic activity of PAP-1 was determined on the *Salmonella typhimurium* tester strains TA97A, TA98, TA100, TA102, and TA1535 by Nelson Laboratories (Salt Lake City, UT).

Receptor Screening. PAP-1 was screened at 1 μM for potential affinity to a panel of 56 receptors by displacement of standard radioligands at MDS Pharma (http://www.mdsps.com). The following receptors were included: adenosine (A_1, A_{2A}, A_3), adrenergic (α_{1A}, α_{1B}, α_{1D}, α_{2A}, β_1, β_2), bradykinin (B_1, B_2), dopamine (D_1, D_{25}, D_3, $D_{4.2}$), endothelin (ET_A, ET_B), epidermal growth factor, estrogen (α), $GABA_A$ (agonist site), $GABA_B$ (benzodiazepine and nonselective), glucocorticoid, glutamate (kainate, NMDA agonism, NMDA glycine, NMDA phencyclidine), histamine (H_1, H_2, H_3), imidazoline (I_2), interleukin-1, leukotriene (CysLT1), muscarinic (M_1, M_2, M_3), neuropeptide Y (Y_1, Y_2), nicotinic acetylcholine, opiate (δ, κ, μ), phorbol ester, platelet activating factor, purinergic (P_{2X}, P_{2Y}), serotonin (5-HT_{1A}, 5-HT_3), σ (σ_1, σ_2), tachykinin (NK_1), testosterone, and transporters (dopamine, GABA, norepinephrine, serotonin). Because significant activity was witnessed only on the dopamine transporter, PAP-1 was retested at 0.01, 0.1, 0.25, and 1 μM to determine an IC_{50} and a Hill coefficient. All assays were performed in duplicate.

Inhibition of Cytochrome P450-Dependent Enzymes. Inhibition of the catalytic activity of purified recombinant human cytochrome P450 2A6 and 3A4 in microsomes (BD Gentest, Woburn, MA) was assayed on the turnover of coumarin (CYP2A6) or 7-benzyloxy-4-trifluoromethyl-coumarin (CYP3A4) by the detection of their fluorescent metabolites (Henderson et al., 1999), and IC_{50} values were determined by testing multiple compound concentrations ranging from 10 nM to 200 μM. All experiments were conducted in duplicate and results are reported as percentage inhibition. Tranylcypromine (CYP2A6) and ketoconazole (CYP3A4) were run as positive controls on the same plates and rendered IC_{50} values of 170 and 37 nM, respectively.

DNA Cross-Linking. The DNA cross-linking potency of selected compounds was determined by measuring melting profiles of poly(dA-dT)-poly(dA-dT) DNA in the presence and absence of compound with and without UVA irradiation according to Dall'Acqua et al. (1971). Incubation mixtures containing 10 μM concentrations of the compound, 0.1 units of poly(dA-dT)-poly(dA-dT) (Sigma-Aldrich, Deisenhofen, Germany), and 1% DMSO and MOPS buffer (0.1 M; pH 7.2) were prepared in 2-ml quartz cuvettes. Samples were irradiated with a Heraeus Fluotest lamp for 30 min at a distance of 20 cm with an intensity of 3.5 mW/cm^2 or stored in the dark for 30 min. Afterward, samples were placed into HP 8845A diode-array spectrophotometer fitted with a Julabo F20-C heating controller. The temperature was directly measured in the cuvettes with a digital thermometer. Heating was applied at a rate of 1°C min^{-1}, with absorbance (260 nm) and temperature data sampling at 1-min intervals until the temperature reached 80°C.

Photoproduction of Singlet Oxygen. The production of singlet oxygen ($^1O_2$) by selected psoralen compounds was determined according to Kraljic and El Moshni (1978). Compound (10 μM) was mixed with 4 μM *N*,*N*-dimethyl-4-nitroso-aniline, 10 mM histidine, and 1% methanol in oxygen-saturated phosphate buffer (0.01 M; pH 7.0) and irradiated with a Heraeus Fluotest lamp for 5 h at a distance of 20 cm with an intensity of 3.5 mW/cm^2. Singlet oxygen mediated photobleaching of the yellow *N*,*N*-dimethyl-4-nitrosoaniline was followed by photometric measurements (440 nm) every 30 min. Results are given as percentage reduction of initial absorption at 440 nM before irradiation and are corrected for "self-bleaching" in the absence of compounds (11.4% ± 0.3%, $n = 9$).

Proliferation Assays. Untouched $CD3^+$ T cells were isolated from peripheral blood of healthy volunteers with RosetteSep (StemCell Technologies, Vancouver, BC, Canada) and then incubated with a biotinylated anti-CCR7 Ab (Clone 3D12; BD PharMingen, San Diego, CA). After two washes with PBS, the labeled cells were first incubated with an anti-biotin tetramer complex (StemCell Technologies) and then with magnetic microbeads. The cells were placed onto a negative selection column in a magnet (all StemCell Technologies) and pure $CCR7^-$ cells were eluted (97% $CCR7^-$ as determined by flow cytometry). $CCR7^-$ T cells were then seeded at 5×10^4 per well together with 5×10^4 autologous irradiated peripheral blood mononuclear cells (PBMCs; 2500 rad) in RPMI culture medium into round-bottomed, 96-well plates. PAP-1 was added at different concentrations, and the cells were stimulated with 25 ng/ml soluble anti-CD3 Ab (Biomeda) 30 min later. To determine the effect of PAP-1 on naive and central memory T cells, human PBMCs were seeded at 2×10^5 cells per well in flat-bottomed, 96-well plates, preincubated with increasing concentrations of PAP-1 for 30 min, and then stimulated with 25 ng/ml anti-CD3 monoclonal Ab (Biomeda, Foster City, CA). [^{3}H]Thymidine (1 μCi/well) was added for the last 12 h of the 60-h assay. Cells were harvested onto glass-fiber filters, and radioactivity was measured in a β-scintillation counter.

DTH. Nine- to 11-week-old female Lewis rats were purchased from Charles River Laboratories (Wilmington, MA) and housed in microisolator cages with irradiated rodent chow and autoclaved water ad libitum. All experiments were in accordance with National Institutes of Health guidelines and approved by the University of California, Davis, Institutional Animal Care and Use Committee. Rats were immunized at the base of the tail with 200 μl of an emulsion of egg albumin grade II (Sigma) in complete Freund's adjuvant (Difco, Detroit, MI). The emulsion was prepared with 50% complete Freund's adjuvant and 50% saline containing a final concentration of 1 mg/ml albumin. Seven days later, the thickness of both ears was measured using a spring-loaded micrometer (Mitutoyo, Spokane, WA). The rats were then challenged by an injection of 10 μl of albumin (2 mg/ml) dissolved in saline in the pinna of one ear and saline in the other ear. In two experiments, rats received i.p. injections of 0.3, 1.0, or 3.0 mg/kg of PAP-1 or of vehicle [saline with 25% Cremophor EL (Sigma)] three times daily for 48 h starting 24 h before the challenge. In another experiment, rats were gavaged three times daily with peanut oil or 5, 20, or 80 mg/kg PAP-1 dissolved in peanut oil (volume 0.5 ml). Ear swelling was measured 24 h later. Values are given as differences in the thickness (μm) of the albumin-injected ear measured before the challenge and 24 h later. The other ear was used as a control for the injection, and the rats were excluded from the experiment if the thickness of the saline-injected ear increased by more than 10%.

Results

Probing of the Alkoxypsoralen Pharmacophore to Increase Selectivity for Kv1.3 over Kv1.5. Using 5-MOP as a template, we previously developed a series of 5-phenyl-

alkoxypsoralens (i.e., Psora series) that inhibited Kv1.3 with low nanomolar affinity (Vennekamp et al., 2004) and found that the essential pharmacophore of this class of Kv1.3 blockers consisted of a psoralen moiety that is attached, through a ~7-Å alkyl chain linker in the 5-position, to a phenyl ring. We further postulated that the Psora compounds bind to the Kv1.3 channel protein via two π-π electron interactions, one involving the psoralen core and the second involving the side chain phenyl ring. Psora-4, the most potent compound of this series, blocked Kv1.3 with an EC_{50} of 3 nM and displayed good selectivity over other Kv channels, except Kv1.5 (EC_{50} 7.7 nM) (Vennekamp et al., 2004). Because Kv1.5 encodes the ultra-rapid delayed rectifier current (I_{Kur}) in the human heart (Fedida et al., 1993), we were concerned about potential cardiac side-effects when using Psora-4 as an immunosuppressant and decided to start a new medicinal chemistry effort centered around Psora-4 to improve the selectivity for Kv1.3 over Kv1.5. Toward this aim, we pursued three synthetic strategies (Fig. 1B). In strategy a, we replaced the side chain phenyl ring with π-electron rich aliphatic substituents or heteroaromatic ring systems. In strategy b**,** we introduced polar functionalities into the linker, such as an ether (O) or a carbonyl (CO) moiety to make the linker more hydrophilic by adding an additional hydrogen acceptor. In strategy c, we planned to alter the electron density in the side-chain phenyl ring by introducing electron-withdrawing or -donating substituents. The chemical identity and purity of all newly synthesized compounds was confirmed by ^{1}H and ^{13}C NMR, mass spectrometry, and combustion analysis before they were tested in whole-cell patch-clamp experiments for their potency to block Kv1.3 and Kv1.5 stably expressed in L929 or MEL cells.

Strategy a: Introduction of π-Electron Rich Aliphatic Substituents or Heteroaromatic Rings. Substitution of the phenyl ring with π-electron–rich aliphatic groups, such as cyano (as in ACP-3) or alkyne (as in AP-1) resulted in a 100- to 1000-fold reduction in potency on Kv1.3 and no significant improvement in selectivity over Kv1.5 (Figs. 1B and 2). This result suggested that in addition to possessing π-electron density, the side chain substituent also has to have a certain minimum bulk. Therefore, we next tried replacing the side chain phenyl ring with bulkier heterocyclic ring systems (Figs. 1B and 2). In general, this strategy rendered compounds of reduced affinity to Kv1.3, and the most obvious conclusion about the structure-activity relationship (SAR) that we could draw from this set of compounds was that the introduction of polar heterocycles, as in PAP-17a and PP-1, or of a basic nitrogen atom (i.e., charged at physiological pH as in PH-3) is extremely detrimental and reduces the affinity of the compounds to Kv1.3 into the low micromolar range. PH-3 constitutes a combination of Psora-4 and the classic K^+ channel blocker 4-aminopyridine in one molecule. Its 4′-amino group (Fig. 1B) is a secondary amine and has a pK_a value of 8.0, meaning that at pH 7.4, roughly 20% of the molecule will exist as the free base and 80% will be protonated. The free base molecules can easily cross the plasma membranes in whole-cell patch-clamp experiments and are likely to be reprotonated at the intracellular pH of 7.2, resulting in only 14% free base and 86% charged molecules in the cytoplasm. Based on this, we postulate that PH-3 is such a weak Kv1.3 blocker because the protonated molecules are unable to bind to the lipophilic alkoxypsoralen binding site, which is very probably located on the intracellular side of the Kv1.3 protein (Wulff et al., 1998; Vennekamp et al., 2004). This hypothesis is supported by the fact that the two pyrimidines PH-9 and PAP-17 (Figs. 1B and 2, top), which are very similar in size and π-electron density to PH-3 but contain no basic nitrogen atom, are much more potent Kv1.3 blockers, with EC_{50} values of 50 and 125 nM, respectively. However, the selectivity of all pyridine- or pyrimidine-substituted compounds over Kv1.5 was extremely poor (0–3-fold).

In contrast, when we replaced the phenyl ring with a 5-membered pyrazole (PH-1; EC_{50}, 450 nM) or thiadiazole ring (PH-4; EC_{50}, 175 nM) or a larger, oxygen-rich coumarin ring (PH-5; EC_{50}, 125 nM), the compounds exhibited 10- to 40-fold selectivity for Kv1.3 over Kv1.5 (Fig. 2, top) despite their ~100-fold loss in activity compared with Psora-4. However, in PH-4 and PH-5, we had also simultaneously introduced an oxygen or a sulfur atom into the side chain right next to the heterocycle, and it was therefore not clear whether the heterocycle or this additional heteroatom in the linker, which constitutes an additional hydrogen bond acceptor, was responsible for the gain in selectivity for Kv1.3 over Kv1.5. To dissect this question, we next synthesized a series of compounds in which we introduced an oxygen atom into the linker but kept the side-chain phenyl ring of Psora-4 intact (Fig. 1B, strategy b).

Strategy b: Introduction of Polar Functionalities into the Linker. The first observation we made when following this strategy was that the compounds were much more potent Kv1.3 blockers (EC_{50} values of 2 to 50 nM) than when we introduced oxygen or sulfur atoms and simultaneously replaced the phenyl ring with heterocycles, demonstrating that a phenyl ring constitutes the optimal ring system in the side chain. Although replacing one of the methylene groups in the linker with a ketone moiety as in KP-1 (Fig. 2, middle) did not improve selectivity over Kv1.5, introduction of an ether oxygen adjacent to the phenyl ring as in PAP-1 (Fig. 2, middle) increased both the potency for Kv1.3 (EC_{50}, 2 nM) and the selectivity over Kv1.5 (EC_{50}, 45 nM). Because PAP-1 was 23-fold selective over Kv1.5, we subsequently synthesized a series of PAPs in which we varied the length of the linker or changed the exact position of the ether oxygen atom (Fig. 2, middle). As with our previously described Psora series (Vennekamp et al., 2004), the potency of the PAP compounds depended on the length of the linker, but the optimal length proved to be ~8 Å, as in PAP-1, instead of ~7 Å, as in Psora-4. Shorter and longer linkers, as in PAP-3 (EC_{50}, 15 nM) and AS-121 (EC_{50}, 15 nM), decreased both potency and selectivity compared with PAP-1 (Fig. 3). Moving the oxygen from position-4 of the linker in PAP-1 to position-3 in PAP-5, PAP-6, and PAP-7 also reduced both potency and selectivity for Kv1.3 (Fig. 2). We therefore concluded that an 8-Å aliphatic linker with an ether oxygen atom adjacent to the phenyl ring constituted an optimum in terms of both potency and selectivity.

Strategy b + c: Introduction of Substituents into the Side-Chain Phenyl Ring of PAP-1. Because PAP-1 exhibited a much higher selectivity for Kv1.3 (EC_{50}, 2 nM) over Kv1.5 (EC_{50}, 45 nM) than Psora-4, we changed our synthetic strategy and altered the π-electron density in the side-chain phenyl ring of PAP-1 instead of Psora-4 as originally planned and thus combined strategies b and c (Figs. 1B and 2). Electron donating groups (-OCH_3, -CH_3, -CF_3) in general slightly

decreased the potency of the compounds on Kv1.3 (EC_{50} values of 7–65 nM) but "destroyed" the selectivity over Kv1.5 (Fig. 2, AS-67, AS-68, AS-96, and AS-118). The effects of electron-withdrawing groups (-NO_2, -Cl) on potency and selectivity were more complicated and depended on the chemical nature of the groups and on the exact position in which they were introduced. The halogen atoms fluorine (AS-111) and chlorine (AS-84) had very little effect on the potency for Kv1.3 with EC_{50} values of 12 and 5 nM, respectively, but drastically reduced the selectivity over Kv1.5 (Fig. 2). Introduction of the strongly electron-withdrawing nitro group in the 4-position as in AS-78 resulted in 15-fold selectivity for Kv1.3 (EC_{50}, 5 nM) over Kv1.5 (EC_{50}, 105 nM) (Fig. 2). However, shifting the nitro group to the 2-position as in PAP-12 (EC_{50}, 61 nM) or to the 3-position as in PAP-13 (EC_{50}, 81 nM) significantly reduced both potency and selectivity (Fig. 3). The introduction of two nitro groups in the 2- and the 4-position as in PAP-14 also did not prove beneficial and further lowered the EC_{50} for Kv1.3 to 140 nM (Fig. 2).

The simultaneous introduction of both an electron-withdrawing nitro group and an electron-donating methoxy (PAP-10) or methyl group (PAP-11) dramatically reduced the potency of the compounds but interestingly reversed the selectivity. Although PAP-10 showed only a marginal preference for Kv1.5, PAP-11 blocked Kv1.5 (EC_{50}, 248 nM) three times more potently than Kv1.3 (EC_{50}, 700 nM). If selective Kv1.5 blockers can be developed out of PAP-11 will be the focus of future experiments, and double substitutions were not pursued further in this SAR study.

Introduction of a bulky phenoxy group in position-4 of the side-chain phenyl ring, as in AS-85 (Fig. 2), decreased the EC_{50} for Kv1.3 by 8-fold to 16 nM but increased the selectivity over Kv1.5 to 45-fold (EC_{50} for Kv1.5, 750 nM). The fact that both the bulky AS-85 (volume 1367 $Å^3$) and the coumarin ring substituted PH-5 (Fig. 1B) displayed such good selectivity suggests that the alkoxypsoralen binding site is wider in Kv1.3 than in Kv1.5. With the synthesis of AS-77, we finally tested the effect of hydration of the furan ring in the psoralen system of PAP-1 and found that it reduced both potency (EC_{50}, 22 nM) and the selectivity (Fig. 2).

PAP-1 and AS-85 Constitute Promising New Kv1.3 Blockers. Of the newly synthesized compounds in this study, PAP-1 constitutes the most promising compound. It inhibits Kv1.3 with an EC_{50} of 2 nM (Fig. 3), exhibits 23-fold selectivity over Kv1.5, and has a logP value of 4.03, and thus the right physicochemical properties to be potentially orally available. Despite its higher selectivity over Kv1.5 (45-fold), the phenoxy-substituted AS-85 is not a good drug candidate, because its high lipophilicity (logP 5.03) violates the Lipinski "rule of five", which states that to be orally available, a potential small-molecule drug should have a molecular weight below 500, a logP value below 5, fewer than five hydrogen bond donors, and fewer than 10 hydrogen bond acceptors (Lipinski et al., 1997). However, its high logP value could make AS-85 an interesting compound for topical application in the treatment of psoriasis and other autoimmune diseases of the skin.

Selectivity of PAP-1 over Other Ion Channels. PAP-1, the most potent of our new compounds, blocked both cloned (EC_{50}, 2.0 ± 0.2 nM) and native Kv1.3 channels in human T cells (EC_{50}, 2.1 ± 0.2 nM) with a Hill coefficient of 2 (Fig. 3B), indicating that two PAP-1 molecules interact with one channel molecule. In contrast to its parent compound Psora-4 (Vennekamp et al., 2004), PAP-1 displayed 23-fold selectivity over the cardiac potassium channel Kv1.5, suggesting that it could be used as an immunosuppressant without causing cardiac side effects. To verify that we did not pick up affinity to any other ion channels while optimizing for selectivity over Kv1.5, we further screened PAP-1 on a panel of 22 K^+, Na^+, Ca^{2+}, and Cl^- channels (Fig. 3C). PAP-1 was found to be 33-fold selective over Kv1.1, 125-fold selective over Kv1.2, 37-fold selective over Kv1.4, 31-fold selective over Kv1.6, and 49-fold selective over Kv1.7. This selectivity over the closely related Kv1-family channels makes PAP-1 the most selective

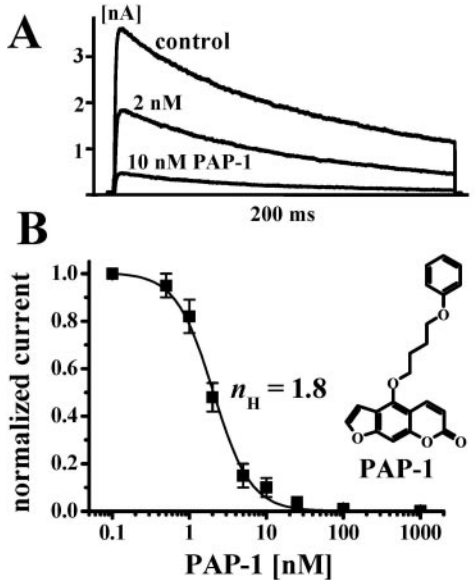

C

	EC_{50} [nM]		EC_{50} [nM]
Kv1.1	65 ± 8	Kv11.1	5000 ± 1000
Kv1.2	250 ± 14	Kir2.1	15 000 ± 1000
Kv1.3	2.0 ± 0.2	KCa1.1	2500 ± 500
Kv1.4	75 ± 5	KCa2.1	10 000 ± 1000
Kv1.5	45 ± 3	KCa2.2	5000 ± 1000
Kv1.6	62 ± 3	KCa2.3	5000 ± 1000
Kv1.7	98 ± 5	KCa3.1	10 000 ± 1000
Kv2.1	3000 ± 500	Nav1.2	7000 ± 1000
Kv3.1	5000 ± 1000	Nav1.4	7000 ± 1000
Kv3.2	980 ± 50	Cav1.2	5000 ± 1000
Kv4.2	1200 ± 100	Cl^-_{swell}	15 000 ± 1000

Fig. 3. A, inhibition of Kv1.3 current by increasing concentrations of PAP-1 in a L929 cell stably expressing Kv1.3. For each concentration equilibrium block after 15 pulses is shown. B, concentration-response curve for PAP-1 on Kv1.3. Each concentration was tested at least three times. C, EC_{50} values of PAP-1 on a panel of 22 cloned and native K^+, Na^+, Ca^{2+}, and Cl^- channels. PAP-1 was tested at three to five concentrations on each channel (n = 3).

known small-molecule Kv1.3 blocker (Chandy et al., 2004). As expected, PAP-1 was even more selective over more distantly related channels: 490-fold over Kv3.2, 600-fold over Kv4.2, and more than 1000-fold over Kv2.1, Kv3.1, Kv11.1 (HERG), the inward-rectifier Kir2.1, the calcium-activated K^+ channels KCa1.1 (BK), KCa3.1 (IKCa1), and $K_{Ca}2.1$–2.3 (SKCa1–3), the neuronal and the skeletal muscle Na^+ channels Nav1.2 and Nav1.4, the voltage-activated Ca^{2+} channel Cav1.2 (L-type), and the swelling-activated chloride channel in human T cells (Fig. 3C).

PAP-1 Binds to the C-Type Inactivated State of Kv1.3. For our template Psora-4, we had previously found that it blocks Kv1.3 by binding to the C-type inactivated state of the channel (Vennekamp et al., 2004) and therefore suspected that PAP-1 would do the same. To test whether PAP-1 blocks the closed Kv1.3 channel or a postactivation state, we first applied a 200-ms depolarizing pulse to elicit a control Kv1.3 current and then perfused 10 nM PAP-1 into the bath while the channel was closed (Fig. 4A). After a 5-min interval to allow ample time for the lipophilic PAP-1 to diffuse into the cell and reach its binding site, we applied a second depolarizing pulse that elicited a current of equivalent amplitude to the control current, confirming our hypothesis that PAP-1 does not bind to the closed channel. With subsequent depolarizing pulses, blockade slowly developed (Fig. 4A), demonstrating that multiple openings of the channel are required to reach steady-state block. This result suggested that PAP-1 blocks either the open and/or C-type inactivated state of Kv1.3. To distinguish between these two possibilities, we performed four types of experiments (Fig. 4, B–F). We first varied the pulse length and found that the time to reach steady-state block depended on the duration of the depolarizing pulse. When depolarizing pulses of 200 ms to 40 mV were applied every 60 s from a holding potential of −80 mV, 900 s (15 pulses) was required to reach steady-state block (Fig. 4B). Lengthening the pulse duration to 2 s and thus causing more of the channels to undergo C-type inactivation during the pulse shortened the time to reach steady-state block to 480 s (8 pulses). In contrast, shortening the pulse duration to 2 ms prolonged the time to reach steady state block to such an extent that 10 nM PAP-1 exhibited less than 10% blockade after ~20 min (Fig. 4C) because under these conditions only a small fraction of the channel ensemble undergoes C-type inactivation. However, the fact that PAP-1 blocks the C-type inactivated state became even more readily apparent when we performed the following experiment: A Kv1.3 control current was elicited through a 200-ms depolarizing pulse from −80 to 40 mV, and the channels were forced into the C-type inactivated state through five consecutive pulses at an interval of 1 s (Fig. 4D). The membrane was then held for 5 min at −80 mV to allow the entire channel ensemble to recover from inactivation. A second set of five consecutive pulses was then applied to again force the channels into the C-type inactivated state, and 10 nM PAP-1 was perfused immediately afterward. After holding the membrane at rest for 5 min, virtually no Kv1.3 channels could be opened because PAP-1 had found them in the C-type inactivated state and blocked them (Fig. 4D). As a final proof that PAP-1 binds to the C-type inactivated state, we studied its effect under conditions in which C-type inactivation was altered, reasoning that this should also change the sensitivity of Kv1.3 to PAP-1. As expected, removal of C-type inactivation by 160 mM external $[K^+]_o$ (Cahalan et al., 1985; Levy and Deutsch, 1996) decreased the potency of PAP-1 by 10-fold compared with 4.5 mM $[K^+]_o$ (Fig. 4E). A similar reduction in potency was seen if C-type inactivation was removed or slowed through mutations in the outer vestibule of Kv1.3 such as H399T (Fig. 4F), H399Y, or A413C (data not shown). In contrast, the A413V mutation, which speeds up inactivation (Panyi et al., 1995), was as sensitive to PAP-1 as the wild-type channel, but equilibrium block was reached faster (data not shown). Taken together, these results indicate that PAP-1 preferentially binds to residues in Kv1.3 that become accessible when the channel undergoes C-type inactivation. The off-binding parameters of PAP-1 were not determined because blockade by PAP-1 was irreversible unless very large volumes of DMSO containing Ringer solution were used for washout.

Toxicity Studies. To determine whether PAP-1 can be safely used in vivo we performed several general toxicity studies and put PAP-1 through an industrial type "Lead Profiling Screen" for selectivity over a panel of 56 receptors. We also more specifically tested for inhibition of P450-dependent enzymes and for photoxicity because some psoralens have been reported to exhibit these properties (Averbeck, 1989; Zhang et al., 2001).

At concentrations ranging from 10 nM to 10 μM, PAP-1 did not reduce the viability of Jurkat T or MEL cells as measured by trypan blue exclusion after 48 h. At a concentration of 1 μM, which corresponds to 500 times the EC_{50} for Kv1.3 blockade, PAP-1 was negative in the Ames test on five tester strains of *Salmonella typhimurium*, demonstrating that it is not mutagenic. In a specificity screen, PAP-1 was tested at 1 μM for displacement of standard radioligands on 56 receptors and transporters. No significant activity was noted on any receptor or transporter except for the human dopamine transporter, stably expressed in Chinese hamster ovary cells on which PAP-1 inhibited binding of the dopamine up-take inhibitor ^{125}I-RTI-55 with an IC_{50} of 100 nM. PAP-1 thus exhibits 50-fold selectivity over the human dopamine transporter and more than 500-fold selectivity over all other tested receptors and transporters. We further injected rats at 60 mg/kg subcutaneously with PAP-1 and witnessed no signs of acute toxicity such as distress, paralysis, ataxia, seizures, or weakness. However, because PAP-1 shows a significant affinity to the human dopamine transporter, we will pay close attention to side effects that might be caused by inhibition of this transporter during future toxicity tests.

Cytochrome P450 Inhibition. Because psoralens such as 8-methoxypsoralen and the related 6′,7′-dihydroxybergamottin, a grapefruit juice constituent, have been reported to inhibit the cytochrome P450 dependent enzymes CYP2A6 or CYP3A4 (Zhang et al., 2001), we tested PAP-1, its hydrated analog AS77, AS-78, PH-9, and 5-MOP for inhibition of these two enzymes (Table 1 for IC_{50} values). Interestingly, all compounds with an aromatic furan ring (PAP-1, AS-78, PH-9, and 5-MOP) showed a higher affinity to CYP3A4, the major xenobiotic metabolizing enzyme in human liver, whereas the hydrated AS-77 preferentially blocked the nicotine metabolizing enzyme CYP2A6 (Table 1). However, compared with the classic CYP3A4 blocker ketoconazole (IC_{50} 37 nM in this assay) and the CYP2A6 blocker tranylcypromine (IC_{50}, 175 nM), all tested psoralens were weak P450 inhibitors. Our most potent Kv1.3 blocker PAP-1 displays more than 1000-

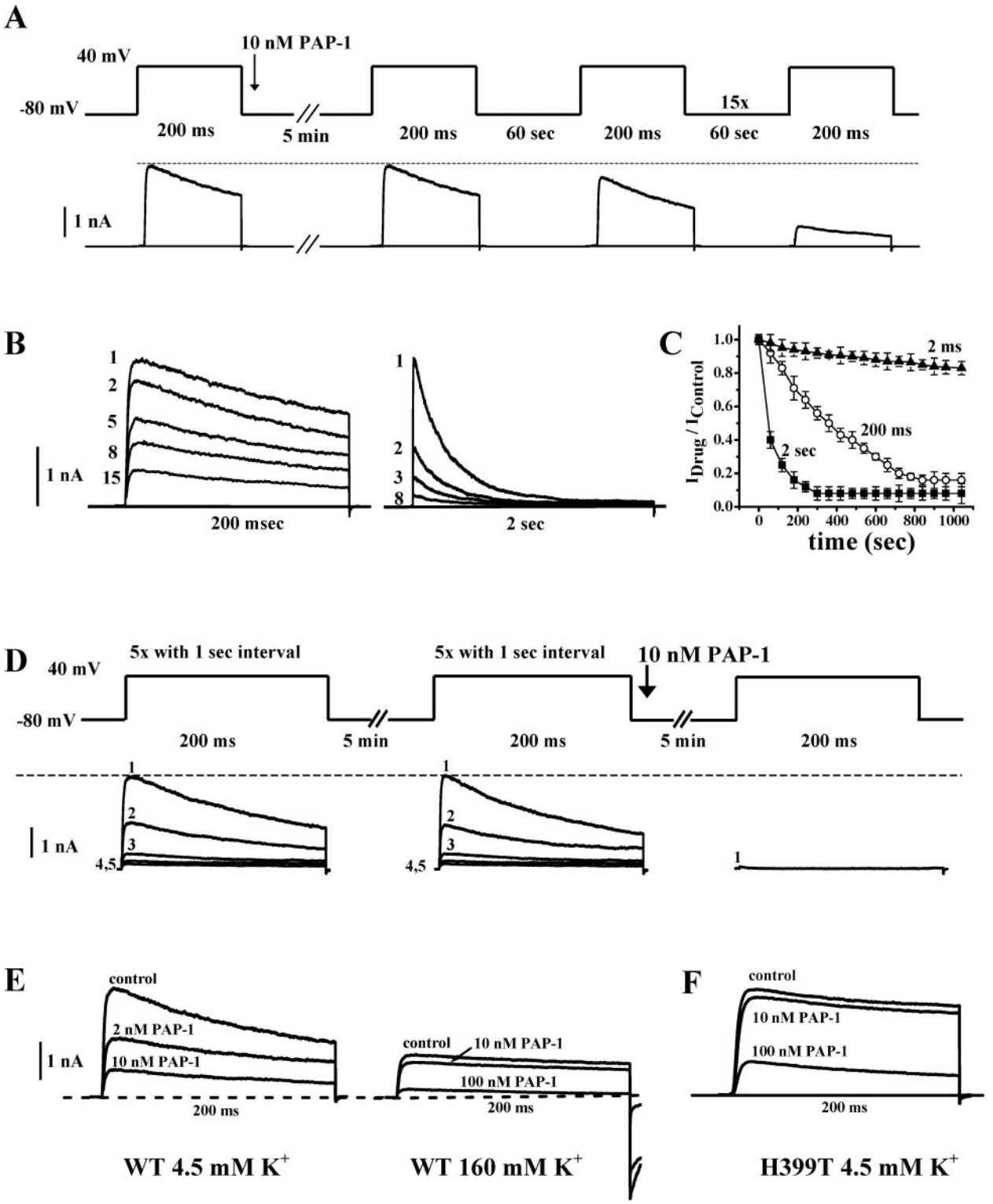

Fig. 4. A, pulse protocol for experiments shown in B. Kv1.3 currents were elicited by a 200-ms depolarizing pulse to 40 mV. PAP-1 (10 nM) was applied to the bath while the membrane was held at −80 mV. After an interval of 5 min, consecutive 2-ms, 200-ms, or 2-s pulses were applied every 60 s. B, inhibition of Kv1.3 by 10 nM PAP-1 during consecutive 200-ms (left) or 2-s pulses (right). The numbers 1 to 15 refer to pulses 1 to 15. C, effect of varying the pulse length from 2 ms to 2 s on time to reach steady-state block. Ordinate, ratio of area under the current curve at various times after start of the consecutive pulses to current before PAP-1 application ($n = 3$). D, Kv1.3 was driven into the C-type inactivated state by five rapid pulses at an interval of 1 s. This pulse protocol was repeated 5 min later to assure that the channel ensemble completely recovered from inactivation in 5 min. PAP-1 (10 nM) was then immediately perfused onto the inactivated channels. After 5 min, we repeated the same rapid pulse protocol. E, effect of changing the external K^+ concentration on the potency of PAP-1 to block WT Kv1.3. Shown are steady-state currents 15 pulses after drug application. F, effect of the H339T mutation in Kv1.3 on the potency of PAP-1.

fold selectivity for Kv1.3 over CYP3A4 (IC_{50}, 2.4 μM) and CYP2A6 (IC_{50}, 45 μM), and it is therefore unlikely that PAP-1 will cause any serious drug-drug interactions in vivo when used in combination with drugs that are metabolized through CYP3A4 or CYP2A6.

Phototoxicity. Depending on the exact orbital configuration of their valence electrons, some psoralens can undergo type 1 and 2 photoreactions with macromolecules in biological systems when irradiated with UVA light (Zarebska, 1994). In type-1 photoreactions (i.e., direct reactions), psoralens form photoadducts with pyrimidine bases of DNA or unsaturated fatty acids in membranes. In type-2 photoreactions, which require the presence of oxygen, psoralen molecules transfer the energy they absorb from UVA light to oxygen and generate reactive oxygen species like singlet oxygen ($^1O_2$), which then oxidize proteins and membrane lipids. Taken together, these reactions underlie the well-known phototoxic, photomutagenic, and photocarcinogenic properties of 5-MOP, 8-MOP, and trioxsalen, which are clinically used for PUVA (psoralen + UVA) therapy of psoriasis (Gasparro, 2000).

DNA Cross-Linking. DNA modification by 8-MOP or trioxsalen is a two-step process in which the planar psoralen system first intercalates into the DNA double helix and then undergoes a photoaddition reaction with a pyrimidine base, preferably thymine, under UVA irradiation (Zarebska, 1994). Because repeated adenine-thymine-sequences are described to be "hot spots" for psoralen cross-linking (Sage and Moustacchi, 1987), we used poly(dA-dT)-poly(dA-dT) DNA to study the photoreactivity of PAP-1. Photobinding of psoralens stabilizes the DNA helix leading to an increase in thermal helix-coil transition temperature (T_m) that corresponds to the amount of cross-linking (Vedaldi et al., 1995). Whereas PAP-1 at 10 μM induced no change in the DNA melting curve ($\Delta T_m = -0.5 \pm 0.3$°C) under UVA irradiation, the classic intercalating psoralens 5-MOP ($\Delta T_m = 12$°C), 8-MOP ($\Delta T_m = 7$°C), and trioxsalen ($\Delta T_m > 28$°C) significantly increased T_m at the same concentration. This result was partly to be expected from PAP-1's structure because psoralens with large substituents are normally too bulky to intercalate into DNA.

Photoproduction of Singlet Oxygen. Singlet oxygen production by psoralens is typically measured through oxidative bleaching of the yellow dye *N*,*N*-dimethyl-*p*-nitrosoanilin (Kraljic and El Moshnie, 1978). In contrast to the strong singlet oxygen producer psoralen (57.4% ± 1.7% bleaching, $n = 4$), we found that PAP-1 at 10 μM was only a very weak producer of singlet oxygen (7.1 ± 0.4% bleaching, $n = 3$). In summary, PAP-1 does not exhibit the photoreactivity of other psoralens and should be free of phototoxic and photomutagenic properties in vivo.

TABLE 1
Inhibition of CYP2A6 and CYP3A4 by selected psoralens
The positive controls were tranylcypromine (CYP2A6) and ketoconazole (CYP3A4).

Compound	IC_{50}	
	CYP2A6 ()	CYP3A4
	μM	
PAP-1	46 ± 7	2.35 ± 0.07
AS-78	>200	5.45 ± 0.08
AS-77	2.1 ± 0.1	>200
PH-9	15 ± 1.4	14.5 ± 0.1
5-MOP	>200	6.85 ± 0.07
Positive control	0.17 ± 0.04	0.037 ± 0.005

PAP-1 Preferentially Suppresses the Proliferation of T_{EM} Cells. Before embarking on in vivo experiments with PAP-1, we tested its effect on the proliferation of human T cells. Similar to its parent compound Psora-4 (Vennekamp et al., 2004) and the Kv1.3 blocking peptides ShK and ShK(L5) (Wulff et al., 2003b; Beeton et al., 2005), we expected that PAP-1 would inhibit the proliferation of $CCR7^-$ T_{EM} cells more potently than the proliferation of bulk peripheral blood T cells that predominantly consist of naive and T_{CM} cells. We therefore isolated $CCR7^-$ T_{EM} cells from $CD3^+$ peripheral blood T cells of three healthy volunteers by eliminating the $CCR7^+$ cells with the help of a biotinylated anti-CCR7 antibody and magnetic beads. The untouched T_{EM} cells, which were confirmed by flow cytometry to be 97% $CCR7^-$, were then stimulated to proliferate with a mitogenic anti-CD3 antibody in the presence and absence of PAP-1. For comparison, we also stimulated PBMCs from the same donors (74–89% $CCR7^+$) with anti-CD3 antibody to elicit a proliferative response that was mainly carried by naive and T_{CM} T cells. We could not use pure $CCR7^+$ cells for these experiments because the anti-CCR7 antibody partially activated the cells that were labeled with it. As shown in Fig. 5A, PAP-1 suppressed the proliferation of T_{EM} with an IC_{50} of 10 nM but was much less effective on PBMCs (IC_{50} ~800 nM), presumably because these cells rapidly up-regulate KCa3.1 during the activation process and thus escape inhibition by Kv1.3 blockers.

PAP-1 Prevents DTH in Lewis Rats. As a final test for whether PAP-1 could be used to target T_{EM} cells in autoimmune reactions, we evaluated its effectiveness in suppressing DTH in Lewis rats. The DTH reaction constitutes a "perfect" model for evaluating Kv1.3 blockers, because it is primarily mediated by skin homing $CD4^+$ T_{EM} cells (Soler et al., 2003). We immunized female Lewis rats with ovalbumin in complete Freund's adjuvant and challenged them 7 days later by an injection of ovalbumin in saline into the pinna of the left ear. The difference in ear thickness was then determined with a micrometer 24 h later as a measure of the immune response against the ovalbumin. PAP-1 or vehicle (saline containing 25% cremophor SL) was i.p. administered three times daily for 48 h starting from the day before the challenge. As shown in Fig. 5B, PAP-1 dose-dependently suppressed the DTH reaction. At 3 mg/kg, PAP-1 was as effective as the peptidic Kv1.3 blocker ShK (16 μg/kg three times daily). PAP-1 also potently suppressed DTH when administered by gavage in peanut oil, demonstrating that it is orally available (Fig. 5C). As is often the case with oral administration, we needed higher doses of PAP-1 to completely suppress DTH and the variations between individual rats were larger presumably because of differences in absorption and metabolism.

Discussion

Using our previously described small molecule Kv1.3 blocker Psora-4 (Vennekamp et al., 2004) as a template, we have further explored the SAR of the phenylalkoxypsoralens and have now identified a number of new phenoxyalkoxypsoralens that potently inhibit the lymphocyte K^+ channel Kv1.3 and display 2 to 50-fold selectivity over the cardiac K^+

channel Kv1.5. Our most "drug-like" new compound, PAP-1, inhibits Kv1.3 with an EC_{50} of 2 nM and is 23-fold selective over Kv1.5. PAP-1 further displays 33- to 125-fold selectivity over all other Kv1-family channels and thus constitutes currently the most potent and selective small molecule Kv1.3 blocker. All other published small molecule Kv1.3 blockers inhibit at least one of the Kv1-channels, most commonly Kv1.4 or Kv1.5, with equal affinity as Kv1.3 (Wulff et al., 2003a; Chandy et al., 2004).

Based on the results presented here and on our previous work, we propose that the essential pharmacophore of the new PAP Kv1.3 blockers consists of a planar, π-electron–rich three-membered ring system that is connected through a roughly 8-Å long linker containing two oxygen atoms to a preferably unsubstituted phenyl ring. Similar to Psora-4, the PAPs probably bind to Kv1.3 via two π-π electron interactions, one involving the psoralen moiety and the second involving the side-chain phenyl ring. Unlike Psora-4, the PAPs contain an additional O atom in the linker, which constitutes a potential additional hydrogen bond acceptor. However, whether or not this O atom really forms a hydrogen bond with the Kv1.3 protein is impossible to say without knowing precisely where the binding site of the PAPs is. A very interesting phenomenon with the PAPs is that the selectivity over Kv1.3 changes from no selectivity to 43-fold selectivity depending on the chemical nature, the size and the exact position of additional substituents on the side-chain phenyl ring. Although the unsubstituted PAP-1 is 23-fold selective over Kv1.5, most substituents with the exception of a strongly electron-withdrawing nitro group in 4-position (AS-78) or the bulky electron donating phenoxy-group (AS-85), reduced the selectivity of PAP-1. Again, without knowing the exact location of the binding site of the PAPs on Kv1.3 and Kv1.5, it is hard to interpret these results, but size seems to be more important than electronic effects in conferring selectivity over Kv1.5. In future studies, we will have to carefully map the binding site of the PAPs on Kv1.3. However, because of the chemical similarity between PAP-1 and correolide, it seems a valid first guess that it might be located in the same area as the correolide binding site in the water-filled inner cavity of Kv1.3 (Hanner et al., 1999, 2001). Although the two binding sites might overlap, we expect that they will not be identical. In contrast to the larger and more lipophilic nortriterpene correolide that binds to Kv1.3 through the comple-

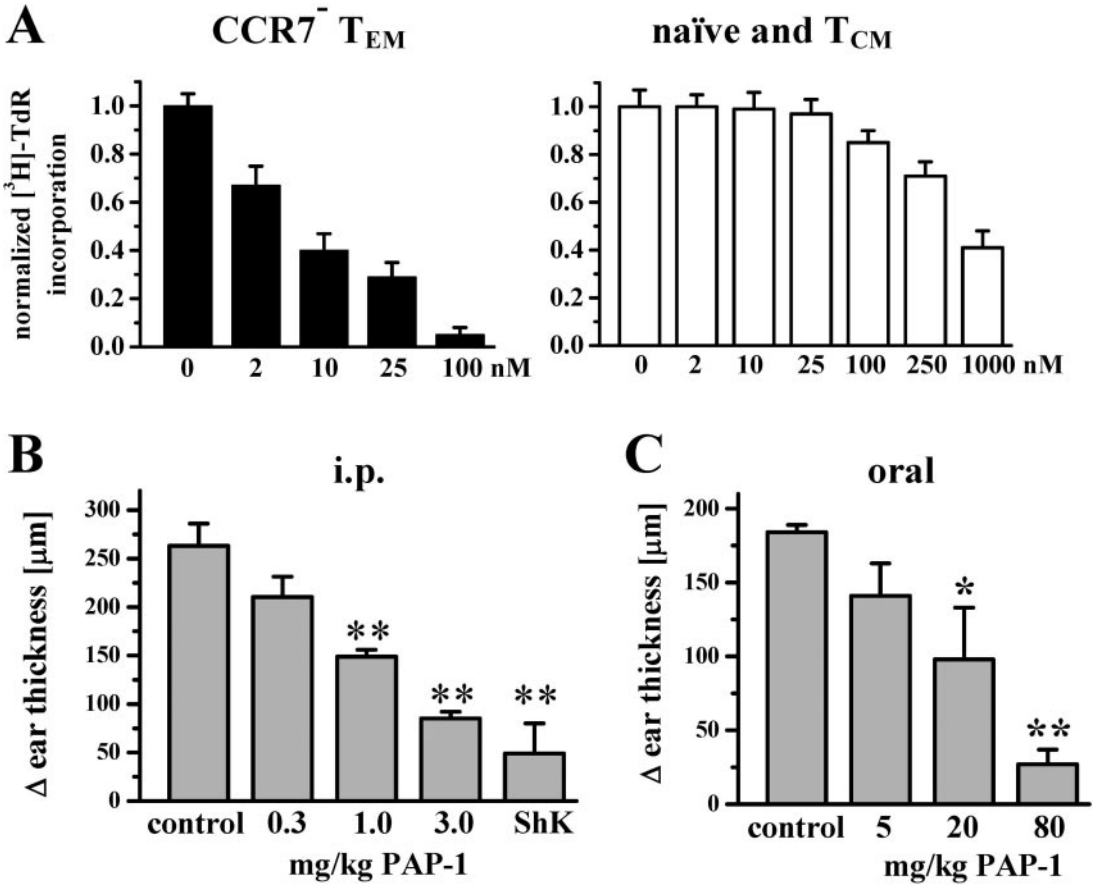

Fig. 5. A, effect of PAP-1 on the anti-CD3 Ab stimulated proliferation of human CCR7$^-$ T_{EM} cells (left) and PBMCs (right). Shown are means ± S.D. from one representative experiment. B, dose-dependent inhibition of DTH reaction by i.p. administration of PAP-1. Shown are the pooled means ± S.E.M. of differences in ear thickness before and 24 h after the challenge from two independent experiments. Vehicle (250 μl of PBS containing 25% cremophor EL), PAP-1, or ShK (16 μg/kg) were injected i.p. three times daily for 48 h. The difference in ear thickness between control (n = 10) and 0.3 mg/kg PAP-1 (n = 8) was not statistically significant (p = 0.13). All other effects were statistically significant: control versus 1.0 mg/kg PAP-1 (n = 7), p = 0.001; control versus 3.0 mg/kg PAP-1 (n = 8), p = 0.00008; control versus ShK (n = 3), p = 0.0009. At 3 mg/kg, PAP-1 is not statistically different from ShK (p = 0.06). C, dose-dependent inhibition of DTH by PAP-1 administered in 500 μl of peanut oil by gavage. Shown are the means ± S.E.M. from one experiment. The difference in ear thickness between control (n = 4) and 5 mg/kg PAP-1 (n = 4) was not statistically significant (p = 0.12). All other effects were statistically significant: control versus 20 mg/kg PAP-1 (n = 3), p = 0.035; control versus 80 mg/kg PAP-1 (n = 3), p = 0.00003.

mentary shape between the bowl-like cavity wall and its own surface, we expect that the PAPs will probably make fewer but "tighter" contacts on the channel involving the two π-electron clouds of the side-chain phenyl ring and the psoralen moiety. Another important difference between correolide and the PAPs consists in their stoichiometry of interaction; correolide has a Hill coefficient of 1, whereas the PAPs exhibit Hill coefficients of 2. We hypothesize that the PAPs bind in the lower region of S5 and S6 and that two molecules "hook" into the channel when the intracellular gate is wide open and lock the channel in the C-type inactivated state.

The good selectivity of PAP-1 over other ion channels, receptors, and transporters, together with its lack of cytotoxicity, mutagenicity, phototoxicity, and acute toxicity in animals, suggests that PAP-1 might indeed be safe for in vivo use. Its low affinity to P450-dependent enzymes also makes it unlikely that PAP-1 should cause any major drug-drug interactions that are mediated through P450 inhibition. PAP-1 could therefore potentially constitute the first small molecule that could be developed into a therapeutically useful immunomodulator. Based on its molecular weight of 350 and its logP value of 4.06, the Lipinski rule of five predicts that PAP-1 should be orally available and, as our oral DTH experiments demonstrate, that this is indeed the case. Compared with Psora-4, the additional O atom in the linker not only increased selectivity over Kv1.5 but also improved the solubility characteristics. Although Psora-4 with a logP value of 4.33 was difficult to dissolve in aqueous solutions despite extensive use of solubilization aids such as ethanol, DMSO, Tween 80, or Cremophor, PAP-1's lower logP of 4.03 made it soluble in physiological saline with the addition of 25% Cremophor. The detailed pharmacokinetics and tissue distribution of PAP-1 will be the focus of future studies by our laboratory. These pharmacokinetic studies in combination with more detailed toxicity studies examining cardiac function will also help us to determine whether the 23-fold selectivity over Kv1.5 is sufficient for safe in vivo use or if selectivity of PAP-1 over Kv1.5 will have to be increased through further derivatization.

PAP-1 potently suppresses the activation of $CCR7^-$ human T_{EM} cells in keeping with the previously described Kv1.3 dependence of these cells (Wulff et al., 2003b; Beeton et al., 2005). In contrast, PAP-1 is much less effective on naive and T_{CM} cells demonstrating its relative selectivity for T_{EM} cells. Because of the crucial role of T_{EM} cells in the pathogenesis of the autoimmune diseases multiple sclerosis, type-1 diabetes, psoriasis, rheumatoid arthritis, and in transplant rejection as well as graft-versus host disease (Beeton and Chandy, 2005), PAP-1 constitutes an attractive new experimental drug for the treatment of these diseases. As a simple model of a T_{EM} cell-mediated immune reaction, we here used DTH and found that PAP-1 effectively prevented this reaction when administered intraperitoneally or orally.

In summary, we here describe the design of the first small-molecule Kv1.3 blocker that is selective over the other Kv1-family channels. This selectivity and PAP-1's effectiveness in suppressing T_{EM} cells both in vitro and in vivo, make PAP-1 an ideal pharmacological tool to further evaluate Kv1.3 as a target for the prevention and treatment of autoimmune diseases in animal models of multiple sclerosis, type-1 diabetes, rheumatoid arthritis, transplant rejection, and graft-versus-host disease. If proven effective in these models and nontoxic in more detailed and more long-term toxicity tests, PAP-1 could potentially be developed into an orally available drug for the treatment of autoimmune diseases.

Acknowledgments

We thank Dieter Heber for expert help with chemical nomenclature, Inga Carstens for the determination of the logP values, Ulrich Giresser for valuable help with NMR and Björn Henke for excellent technical assistance.

References

Averbeck D (1989) Recent advances in psoralen phototoxicity mechanism. *Photochem Photobiol* **50:**859–882.

Bardien-Kruger S, Wulff H, Arieff Z, Brink P, Chandy KG, and Corfield V (2002) Characterization of the human voltage-gated potassium channel gene, KCNA7, a candidate gene for inherited cardiac disorders and its exclusion as a cause of progressive familial heart block I (PFHBI). *Eur J Human Gen* **10:**36–43.

Beeton C, Barbaria J, Giraud P, Devaux J, Benoliel A, Gola M, Sabatier J, Bernard D, Crest M, and Beraud E (2001a) Selective blocking of voltage-gated K^+ channels improves experimental autoimmune encephalomyelitis and inhibits T cell activation. *J Immunol* **166:**936–944.

Beeton C and Chandy KG (2005) Potassium channels, memory T cells and multiple sclerosis. *Neuroscientist,* in press.

Beeton C, Pennington MW, Wulff H, Singh S, Nugent D, Crossley G, Khaytin I, Calabresi PA, Chen CY, Gutman GA, et al. (2005) Targeting effector memory T cells with a selective peptide inhibitor of Kv1.3 channels for therapy of autoimmune diseases. *Mol Pharmacol* **67:**1369–1381.

Beeton C, Wulff H, Barbaria J, Clot-Faybesse O, Pennington M, Bernard D, Cahalan MD, Chandy KG, and Beraud E (2001b) Selective blockade of T lymphocyte K^+ channels ameliorates experimental autoimmune encephalomyelitis, a model for multiple sclerosis. *Proc Natl Acad Sci USA* **98:**13942–13947.

Bohuslavizki KH, Hansel W, Kneip A, Koppenhofer E, Niemoller E, and Sanmann K (1994) Mode of action of psoralens, benzofurans, acridones and coumarins on the ionic currents in intact myelinated nerve fibres and its significance in demyelinating diseases. *Gen Physiol Biophys* **13:**309–328.

Bohuslavizki KH, Hinck-Kneip C, Kneip A, Koppenhofer E, and Reimers A (1993) Reduction of MS-related scotoma by a new class of potassium channel blockers from *Ruta graveolens*. *Neuroopthalmol* **13:**191–198.

Cahalan MD, Chandy KG, DeCoursey TE, and Gupta S (1985) A voltage-gated potassium channel in human T lymphocytes. *J Physiol (Lond)* **358:**197–237.

Chandy KG, Wulff H, Beeton C, Pennington M, Gutman GA, and Cahalan MD (2004) Potassium channels as targets for specific immunomodulation. *Trends Pharmacol Sci* **25:**280–289.

Dall'Acqua F, Marciani S, Ciavetta L, and Rodighiero G (1971) Formation of interstrand cross-links in the photoreactions between furocoumarins and DNA. *Z. Naturforsch* **26b:**561–569.

Dorner T and Lipsky PE (2004) Correlation of circulating CD27high plasma cells and disease activity in systemic lupus erythematosus. *Lupus* **13:**283–289.

Fasth AE, Cao D, van Vollenhoven R, Trollmo C, and Malmstrom V (2004) CD28nullCD4+ T cells—characterization of an effector memory T-cell population in patients with rheumatoid arthritis. *Scand J Immunol* **60:**199–208.

Fedida D, Wible B, Wang Z, Fermini B, Faust F, Nattel S, and Brown A (1993) Identity of a novel delayed rectifier current from human heart with a cloned K^+ channel current. *Circ Res* **73:**210–216.

Gasparro FP (2000) The role of PUVA in the treatment of psoriasis. Photobiology issues related to skin cancer incidence. *Am J Clin Dermatol* **1:**337–348.

Grissmer S, Dethlefs B, Wasmuth JJ, Goldin AL, Gutman GA, Cahalan MD, and Chandy KG (1990) Expression and chromosomal localization of a lymphocyte K^+ channel gene. *Proc Natl Acad Sci USA* **87:**9411–9415.

Grissmer S, Nguyen AN, Aiyar J, Hanson DC, Mather RJ, Gutman GA, Karmilowicz MJ, Auperin DD, and Chandy KG (1994) Pharmacological characterization of five cloned voltage-gated K^+ channels, types Kv1.1, 1.2, 1.3, 1.5 and 3.1, stably expressed in mammalian cell lines. *Mol Pharmacol* **45:**1227–1234.

Gutman GA, Chandy KG, Adelman JP, Aiyar J, Bayliss DA, Clapham DE, Covarriubias M, Desir GV, Furuichi K, Ganetzky B, et al. (2003) International Union of Pharmacology. XLI. Compendium of voltage-gated ion channels: potassium channels. *Pharmacol Rev* **55:**583–586.

Hanner M, Green B, Gao Y-D, Schmalhofer W, Matyskiela M, Durand DJ, Felix JP, Linde A-R, Bordallo C, Kaczorowski GJ, et al. (2001) Binding of correolide to the Kv1.3 potassium channel: characterization of the binding domain by site-directed mutagenesis. *Biochemistry* **40:**11687–11697.

Hanner M, Schmalhofer WA, Green B, Bordallo C, Liu J, Slaughter RS, Kaczorowski GJ, and Garcia ML (1999) Binding of correolide to Kv1 family potassium channels. *J Biol Chem* **274:**25237–25244.

Hansen A, Odendahl M, Reiter K, Jacobi AM, Feist E, Scholze J, Burmester GR, Lipsky PE, and Dorner T (2002) Diminished peripheral blood memory B cells and accumulation of memory B cells in the salivary glands of patients with Sjogren's syndrome. *Arthritis Rheum* **46:**2160–2171.

Hanson DC, Nguyen A, Mather RJ, Rauer H, Koch K, Burgess LE, Rizzi JP, Donovan CB, Bruns MJ, Canniff PC, et al. (1999) UK-78,282, a novel piperidine compound that potently blocks the Kv1.3 voltage-gated potassium channel and inhibits human T cell activation. *Br J Pharmacol* **126:**1707–1716.

Henderson GL, Harkey MR, Gershwin ME, Hackman RM, Stern JS, and Stressser DM (1999) Effects of gingseng components on c-DNA-expressed cytochrome P450 enzyme catalytic activity. *Life Sci* **65:**PL209–214.

Kolski-Andreaco A, Tomita H, Shakkottai VG, Gutman GA, Cahalan MD, Gargus JJ,

and Chandy KG (2004) SK3–1C, a dominant-negative suppressor of SKCa and IKCa channels. *J Biol Chem* **279:**6893–6904.
Kraljic I and El Moshnie SE (1978) A new method for the detection of singlet oxygen in aqueous solution. *Photochem Photobiol* **28:**577–581.
Levy DI and Deutsch C (1996) Recovery from C-type inactivation is modulated by extracellular potassium. *Biophys J* **70:**798–805.
Lipinski CA, Lombardo F, Dominy BW, and Feeney PJ (1997) Experimental and computational approaches to estimate solubility and permeability in drug discovery and development settings. *Adv Drug Delivery Rev* **23:**3–25.
Markovic-Plese S, Cortese I, Wandinger KP, McFarland HF, and Martin R (2001) $CD4^+CD28^-$ costimulation-independent T cells in multiple sclerosis. *J Clin Investig* **108:**1185–1194.
Nguyen A, Kath JC, Hanson DC, Biggers MS, Canniff PC, Donovan CB, Mather RJ, Bruns MJ, Rauer H, Aiyar J, et al. (1996) Novel nonpeptide agents potently block the C-type inactivated conformation of Kv1.3 and suppress T cell activation. *Mol Pharmacol* **50:**1672–1679.
Panyi G, Sheng Z, and Deutsch C (1995) C-type inactivation of a voltage-gated K^+ channel occurs by a cooperative mechanism. *Biophys J* **69:**896–903.
Pearl JP, Parris J, Hale DA, Hoffmann SC, Bernstein WB, McCoy KL, Swanson SJ, Mannon RB, Roederer M, and Kirk AD (2005) Immunocompetent T-cells with a memory-like phenotype are the dominant cell type following antibody-mediated T-cell depletion. *Am J Transplant* **5:**465–474.
Ross PE, Garber SS, and Cahalan MD (1994) Membrane chloride conductance and capcitance in Jurkat T lymphocytes during osmotic swelling. *Biophys J* **66:**169–178.
Sage E and Moustacchi E (1987) Sequence context effects on 8-methoxypsoralen photobinding to defined DNA fragments. *Biochemistry* **26:**3307–3314.
Schmalhofer WA, Bao J, McManus OB, Green B, Matyskiela M, Wunderler D, Bugianesi RM, Felix JP, Hanner M, Linde-Arias A-R, et al. (2002) Identification of a new class of inhibitors of the voltage-gated potassium channel, Kv1.3, with immunosuppressant properties. *Biochemistry* **18:**7781–7794.
Schoenberg A and Aziz G (1953) Furochromones and Coumarins. VI. Demethylation of xanthotoxin, khellin and khellol with aniline hydrochloride and magnesium iodide. *Am J Chem Soc* **75:**3265–3266.
Singh SB, Zink DL, Dombrowski AW, Dezeny G, Bills GF, Felix JP, Slaughter RS, and Goetz MA (2001) Candelalides A-C: novel diterpenoid pyrones from fermentations of *Sesquicillium candelabrum* as blockers of the voltage-gated potassium channel Kv1.3. *Org Lett* **3:**247–350.
Soler D, Humphreys TL, Spinola SM, and Campbell JJ (2003) CCR4 versus CCR10 in human cutaneous TH lymphocyte trafficking. *Blood* **101:**1677–1682.
Vedaldi D, Caffieri S, Frank S, Dall'Acqua F, Jakobs A, and Piette J (1995) Sulphur and selenium analogues of psoralen as novel potential photochemotherapeutic agents. *Farmaco* **50:**527–536.
Vennekamp J, Wulff H, Beeton C, Calabresi PA, Grissmer S, Hansel W, and Chandy KG (2004) Kv1.3 blocking 5-phenylalkoxypsoralens: a new class of immunomodulators. *Mol Pharmacol* **65:**1364–1373.
Viglietta V, Kent SC, Orban T, and Hafler DA (2002) GAD65-reactive T cells are activated in patients with autoimmune type 1a diabetes. *J Clin Investig* **109:**895–903.
Vissers WH, Arndtz CH, Muys L, Van Erp PE, de Jong EM, and van de Kerkhof PC (2004) Memory effector (CD45RO+) and cytotoxic (CD8+) T cells appear early in the margin zone of spreading psoriatic lesions in contrast to cells expressing natural killer receptors, which appear late. *Br J Dermatol* **150:**852–859.
Wermuth CG (2004) Selective optimization of side activities: another way for drug discovery. *J Med Chem* **47:**1303–1314.
Wernekenschnieder A, Korner P, and Hansel W (2004) 3-Alkyl- and 3-aryl-7H-furo[3,2-*g*]chromen-7-ones as blockers of the voltage-gated potassium channel Kv1.3. *Pharmazie* **59:**319–320.
Wulff H, Beeton C, and Chandy KG (2003a) Potassium channels as therapeutic targets for autoimmune disorders. *Curr Opin Drug Discov Devel* **6:**640–647.
Wulff H, Calabresi PA, Allie R, Yun S, Pennington M, Beeton C, and Chandy KG (2003b) The voltage-gated Kv1.3 K^+ channel in effector memory T cells as new target for MS. *J Clin Investig* **111:**1703–1713.
Wulff H, Knaus HG, Pennington M, and Chandy KG (2004) K^+ channel expression during B-cell differentiation: implications for immunomodulation and autoimmunity. *J Immunol* **173:**776–786.
Wulff H, Miller MJ, Haensel W, Grissmer S, Cahalan MD, and Chandy KG (2000) Design of a potent and selective inhibitor of the intermediate-conductance Ca^{2+}-activated K^+ channel, IKCa1: A potential immunosuppressant. *Proc Natl Acad Sci USA* **97:**8151–8156.
Wulff H, Rauer H, During T, Hanselmann C, Ruff K, Wrisch A, Grissmer S, and Haensel W (1998) Alkoxypsoralens, novel nonpeptide blockers of Shaker-type K^+ channels: synthesis and photoreactivity. *J Med Chem* **41:**4542–4549.
Yamashita K, Choi U, Woltz PC, Foster SF, Sneller MC, Hakim FT, Fowler DH, Bishop MR, Pavletic SZ, Tamari M, et al. (2004) Severe chronic graft-versus-host disease is characterized by a preponderance of $CD4^+$ effector memory cells relative to central memory cells. *Blood* **103:**3986–3988.
Zarebska Z (1994) Cell membrane, a target for PUVA therapy. *J Photochem Photobiol B* **23:**101–109.
Zhang W, Kilicarslan T, Tyndale RF, and Sellers EM (2001) Evaluation of methoxsalen, tranylcypromine and tryptamine as specific and selective CYP2A6 inhibitors in vitro. *Drug Metab Dispos* **29:**897–902.
Zhou Z, Gong Q, Ye B, Fan Z, Makielski JC, Robertson GA, and January CT (1998) Properties of HERG channels stably expressed in HEK 293 cells studied at physiological temperatures. *Biophys J* **74:**230–241.

Address correspondence to: Heike Wulff, Department of Medical Pharmacology and Toxicology, Genome and Biomedical Sciences Facility, Room 3502, 451 East Health Sciences Drive, University of California, Davis, Davis, CA 95616. E-mail: hwulff@ucdavis.edu.